

# final report

Project code: P.PSH.0747

Prepared by: Victor Martchenko, Jonathan Cook, Merv Shirazi  
Scott Automation and Robotics

Date published: 20 December 2016

PUBLISHED BY  
Meat and Livestock Australia Limited  
Locked Bag 991  
NORTH SYDNEY NSW 2059

## Hyperspectral Food Safety Inspection System

### Final Report

Meat & Livestock Australia acknowledges the matching funds provided by the Australian Government to support the research and development detailed in this publication.

This publication is published by Meat & Livestock Australia Limited ABN 39 081 678 364 (MLA). Care is taken to ensure the accuracy of the information contained in this publication. However MLA cannot accept responsibility for the accuracy or completeness of the information or opinions contained in the publication. You should make your own enquiries before making decisions concerning your interests. Reproduction in whole or in part of this publication is prohibited without prior written consent of MLA.

## Abstract

With the current growing need for low production costs and high efficiency, the food industry is faced with a number of challenges, including maintenance of high quality standards and assurance of food safety while avoiding liability issues. A hyperspectral camera with a large spectral range (400-2500nm) was purchased to investigate its ability to detect contaminations of interest linking to food safety issues such as ingesta, faeces, bile, urine, *Salmonella*, *E. coli* and *Listeria*. While some success was achieved with all contaminants, ingesta and faeces were the most successful. These were also deemed to be of high value to industry as importing countries use them as hygiene indicators. The second set of trials conducted focussed on ingesta and faeces. Detection algorithms were developed using two different analysis methodologies, both yielding high levels of accuracy - up to 99.67% success rate for classification of pixels as contamination, fat or lean pixels in the hyperspectral image. The algorithms were built focussing on a number of key wavelengths, particularly within the 450-750nm and 900-1450nm ranges.

While challenges still exist to transition to commercial scale, it is believed that the hyperspectral imaging technology is suitable for performing on-line detection of faeces and ingesta contamination on red meat products.

It is recommended that the results and algorithms developed in this project should be built upon by conducting further trials examining a larger sample size to improve accuracy, demonstrate robustness in coping with variations in carcass factors (e.g. area of the carcass, breed, feed type) and help develop a commercially viable concept system.

## Executive Summary

Hyperspectral imaging technology presents a unique opportunity to the red meat industry, particularly in the area of food safety. This project aimed to investigate the use of the technology in this area. A hyperspectral camera was selected and purchased. This camera possesses a large spectral range (400-2500nm) which gave flexibility in assessing the wavelengths of interest for the range of applications being assessed.

A series of experiments were conducted to investigate a number of food safety applications using the technology on contamination such as ingesta, faeces, bile and urine. A number of microbiological contaminants were also investigated – *Salmonella*, *E. coli* and *Listeria*.

Uncontaminated meat was obtained from a processor, which was scanned with the hyperspectral camera to assess the amount of natural variation occurring within the spectral data for muscle and fat. This meat was obtained from the neck area of the carcass as this area is particularly vulnerable to contamination. While a significant amount of variation was found between samples, common features were able to be identified which can be used to characterise 'fat' and 'lean', with lean exhibiting less variation than fat.

A series of controlled trials were then performed using varying amounts of the aforementioned contaminants. Furthermore, the trials were conducted using standard white lighting, as well as ultraviolet (UV) lighting. The reason for this is that some substances fluoresce when excited with UV light. This was identified as another potential mechanism to identify the contaminants of interest.

The initial trials demonstrated that ingesta and faeces detection gave promising results and was identifiable on both muscle and fat tissue. Urine and bile detection seemed more difficult but was able to be identified in high concentrations. It is thought that one of the issues lies in the fact that urine and bile get absorbed by the meat, thus making detection more difficult. Further investigations are required for these contaminants. Tests of the microbiological samples were also rather challenging and require further testing. One potential opportunity may be in performing time-lapse trials to assess if their detection becomes possible over certain time periods. Some other challenges experienced were due to the limitations of the camera. While possessing an excellent spectral range and resolution, the camera is relatively slow and has a small spatial resolution resulting in large pixels (approximately 0.5mm long in the travel direction by 2mm wide). The implications of these factors result in motion blurring as well as partial volume effects which can make it difficult to effectively characterise each pixel accurately. These challenges were able to be overcome quite well for the ingesta and faeces applications in particular.

A second set of trials was then conducted focussing on detection of ingesta and faeces contamination. Contamination was diluted to a number of different concentrations (12.5%, 25%, 50%, 100%) and coated on muscle and fat surfaces of meat samples. The results were then analysed and algorithms were developed, using a decision tree analysis and a discriminant multivariate analysis. Both methods yielded high levels of accuracy in identifying both forms of contamination, even at the most diluted concentration of 12.5%. The decision tree analysis method was able to successfully flag both contaminated muscle

and fat tissue surfaces. The discriminant analysis algorithms were assessed at a pixel level, achieving a success rate of above 99.5% for both faeces and ingesta. The contamination was brushed onto the entire surface of the meat. It can be seen that, while there are certainly areas where contamination is visible to the eye, there are also areas on the meat where it is not. The detection algorithms flagged almost the entire surface as being contaminated on a pixel-by-pixel basis, demonstrating that the algorithms can classify contamination which isn't visible to the human eye. If further trials are conducted, a method can be used whereby ingesta and faeces samples are dehydrated, crushed then reconstituted with the same amount of water lost to demonstrate further the ability of the system to detect contamination not visible to the human eye. Alternatively, large fibrous material could be sieved from the samples.

While challenges still exist to transition to commercial scale, it is believed that the hyperspectral imaging technology is suitable for performing on-line detection of faeces and ingesta contamination on red meat products.

It is recommended that, using the learnings from this project, a larger set of trials can be designed to further test and improve these algorithms for a larger sample size. Such a trial would cover variations such as carcass breed, feed type etc. A commercially feasible concept could then be designed for hyperspectral detection of ingesta and faeces contamination of carcasses.

## Table of Contents

1	Background.....	7
2	Project objectives.....	8
2.1	Objective 1:.....	8
2.2	Objective 2:.....	8
2.3	Objective 3:.....	8
3	Hardware Selection and System Build .....	8
4	Trials Stage 1 – Initial testing .....	9
4.1	Trial one – Testing the natural spectral variation in protein and fat.....	9
4.1.1	Aim .....	9
4.1.2	Method.....	9
4.1.3	Results.....	11
4.1.3.1	Lean/Protein Spectra deviation .....	11
4.1.3.2	Fat Spectral Deviation.....	12
4.1.4	Conclusion .....	13
4.2	Trial two – investigating small amounts of contamination .....	14
4.2.1	Aim .....	14
4.2.2	Method.....	14
4.2.3	Results.....	15
4.2.4	Conclusion .....	17
4.3	Trial three – Microbiological contamination .....	17
4.3.1	Aim .....	17
4.3.2	Method.....	18
4.3.3	Results.....	18
4.3.4	Conclusions .....	19
4.4	Trial four – effect of UV lighting.....	19
4.4.1	Aim .....	19
4.4.2	Method.....	20
4.4.3	Results.....	20
4.4.4	Conclusion .....	21
5	Trials Stage 2 – Focused trials (ingesta and faeces).....	22
5.1	Aim .....	22

5.2	Method.....	22
5.3	Results.....	27
5.3.1	Contaminant spectra.....	27
5.3.1.1	Faeces spectra .....	27
5.3.1.2	Ingesta spectra .....	29
5.3.1.3	Combination .....	30
5.3.2	Diluted contaminants .....	31
5.3.2.1	Sample 1 faeces with 100% contamination.....	31
5.3.2.2	Sample 2 faeces with 50% contamination dilution.....	32
5.3.2.3	Sample 3 faeces with 25% contamination dilution.....	33
5.3.2.4	Sample 4 faeces with 12.5% contamination dilution.....	34
5.3.2.5	Sample 5 ingesta with 100% contamination.....	35
5.3.2.6	Sample 6 ingesta with 50% contamination dilution.....	36
5.3.2.7	Sample 7 ingesta with 25% contamination dilution.....	37
5.3.2.8	Sample 8 ingesta with 12.5% contamination dilution.....	38
5.3.3	Conclusions .....	39
5.4	Secondary Analysis .....	39
5.4.1	Ingesta.....	39
5.4.2	Faeces.....	45
5.4.3	Combined model.....	48
5.4.4	Conclusions .....	51
6	Conclusions and Recommendations.....	51
	Appendix A – Initial trial Results Register.....	53

# 1 Background

With the current need for low production costs and high efficiency, the food industry is faced with a number of challenges, including maintenance of high quality standards and assurance of food safety while avoiding liability issues. Meeting these challenges has become crucial in regards to grading food products (for quality and safety) for different markets. Food companies and suppliers need efficient, low cost and non-invasive quality and safety inspection technologies to enable them to satisfy different markets' needs, thereby raising their competitiveness and expanding their market share.

With recent advancements in computer technology and instrumentation engineering, there have been significant advancements in techniques for food quality and safety. Machine vision and NIR spectroscopy are two of the more extensively applied methods for food safety and food quality assessment.

Machine vision techniques based on red-green-blue (RGB) colour vision systems have been successfully applied to evaluate the external characteristics of foods. Normal machine vision systems are not able to capture broad spectral information which is related to internal characteristics; hence computer vision has limited ability to conduct quantitative analysis of chemical components in food.

Spectroscopy is a popular analytical method for quantification of the chemical components of food.

The tight relationship between NIR spectra and food components makes NIR spectroscopy more attractive than other spectroscopy techniques. However, these spectral methods were proven to be inefficient when it comes to heterogeneous materials such as meat, owing to the fact that they are not capable of obtaining any spatial information about objects.

Due to the limitations of regular machine vision and spectroscopy techniques (such as NIR), hyperspectral imaging was developed. Hyperspectral imaging can be used to obtain spectral and spatial information of an object over the ultraviolet, visible and near-infrared regions (300 – 2600nm).

Recently the hyperspectral technique has become more and more popular in food quality control in order to meet consumer demands and the challenge of market segmentation and legal restrictions.

This project will work with a selectable wavelength hyperspectral camera to ascertain which are the optimum wavelengths required for detecting a number of contaminants.

## 2 Project objectives

### 2.1 Objective 1:

Identify which areas of focus and contamination combinations can be identified using Hyperspectral technology platform, in a value adding way to the meat processing sector.

### 2.2 Objective 2:

Identify how any successful findings from this project can be commercially scaled up.

### 2.3 Objective 3:

Proposal developed for commercial system (where applicable) for subsequent phases (in conjunction with MLA).

## 3 Hardware Selection and System Build

A review was completed on various hyperspectral cameras to decide which should be purchased for the purposes of these trials. The Specim AsiaFENIX was selected due to its wide spectral range (380 – 2500nm). Similarly, a range of data processing software packages were reviewed to process the hyperspectral data obtained during the trials. Envi was selected due to its substantial user base, large array of spectral transformation and classification algorithms, good representation in Australia and its ability to be expanded upon using IDL (Interactive Data Language).

Lighting was also purchased and a scanning rig constructed to enable samples to be scanned by the hyperspectral camera. Ultraviolet lights were also purchased in order to trial their potential to assist in robust contamination detection using the hyperspectral camera.

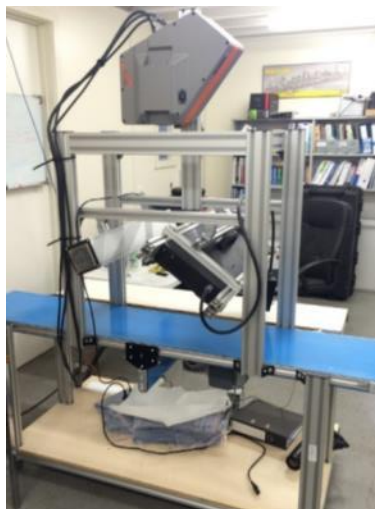


Figure 1 - Camera testing rig.



## 4 Trials Stage 1 – Initial testing

Once the camera was setup, training sessions were carried out to familiarise SCOTT engineers with the hardware and software purchased. These training sessions included performing some initial trials on meat samples to understand the specific workings and challenges associated with the context of this project. From this, a scope and trialling plan was developed for the next milestones of the project.

It was agreed that the following contaminants should be examined: ingesta, faeces, bile and urine. Microbiological contamination was also to be examined, with the focus being on *Listeria*, *E. coli* and *Salmonella*.

### 4.1 Trial one – Testing the natural spectral variation in protein and fat

#### 4.1.1 Aim

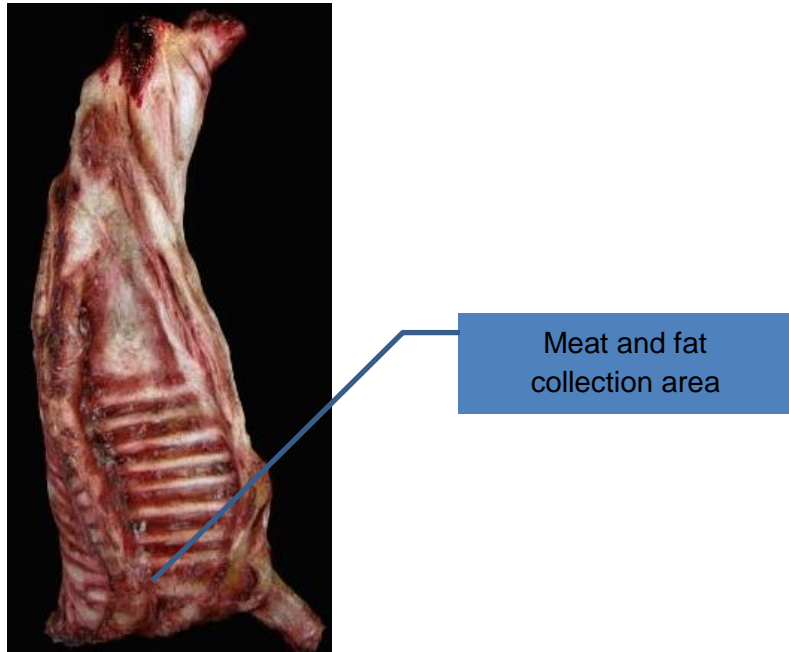
From earlier experiments conducted throughout the project it was found that there is quite a large amount of variation in the spectra of fat and protein on various red meat products. A lot of these variations can be attributed the natural variation of each animal.

Contamination that is difficult or impossible to see in the visible spectra may be visible in some of the invisible wavelengths of lighting. The effect of contamination on spectra for clean protein or fat can be large when there is a large concentration of contamination on the surface. However, when there is a very small amount of contaminant, the effect on the spectra will be minimal. To detect small variation on a surface that is not naturally variable is an identified risk which must be evaluated.

Prior to detecting very small spectral change on the surface of the product, it was necessary to understand what kind of spectral deviation can be expected from a controlled production run. The aim of this experiment was to measure and document the natural spectral variation on the surface of the carcass in a small production run in a meat processing plant. The desired outcome of the experiment was to understand how small a spectral change will need to be to become detectable (within the operating wavelength of our equipment) in a herd of animals.

#### 4.1.2 Method

30 samples were gathered from the processing floor at a processing plant. The samples were collected from the neck area of each carcass (Figure 2Figure 1). A sample of roughly 100g was collected from each carcass. Each sample was placed into a separate plastic container to avoid cross contamination. Knives were sterilised between samples.



**Figure 2 – Side of beef. The area for the carcass of where samples were collected**

The following scanning methodology was then applied:

- The camera exposure and lighting settings were configured so that the maximum intensity of the spectra on the Spectralon plate is at 70 percent of the capability of the camera.
- A white and dark calibration image were acquired.
- Each sample was scanned individually with a constant conveyer speed. Each data cube was saved with a timestamp.
- Samples were discarded and equipment sterilised with alcohol.
- Each sample was individually analysed.
  - A mean spectrum was collected using a region of interest (ROI) on clean portions of meat and fat. Figure 3 shows an example of RIO selection. The spectra were saved to separate CSV file with a file name being the timestamp of the original data file for traceability.
  - ROI for the mean spectrum was selected on the clearest part of the image with no deep cavities that could cast a shadow.

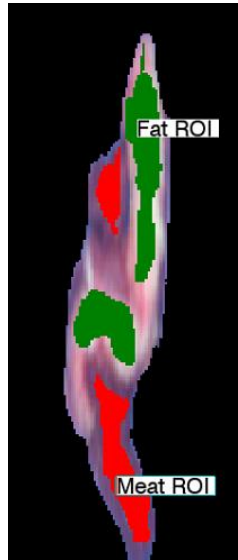


Figure 3 – Image of Region of Interest select on Sample number 13.

#### 4.1.3 Results

##### 4.1.3.1 *Lean/Protein Spectra deviation*

All lean samples were collected, scanned and analysed. To gain an understanding of what kind of spectral deviation can be expected, all of the data is represented on one graph. Please refer to Figure 4 and Figure 5 for a representation of the encountered spectra.

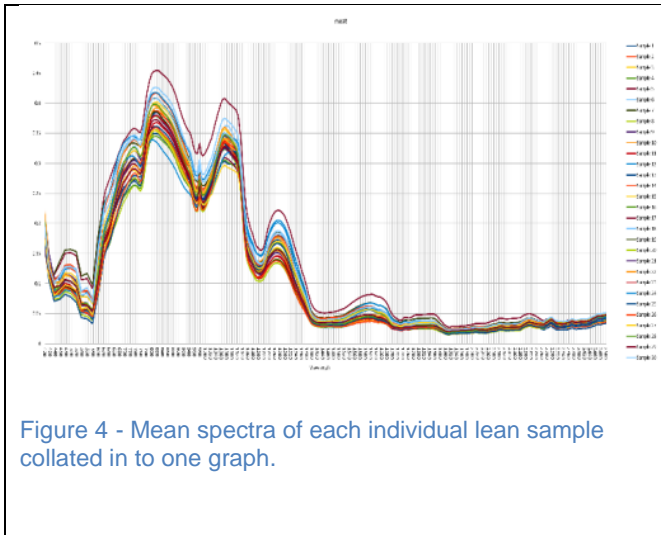


Figure 4 - Mean spectra of each individual lean sample collated in to one graph.

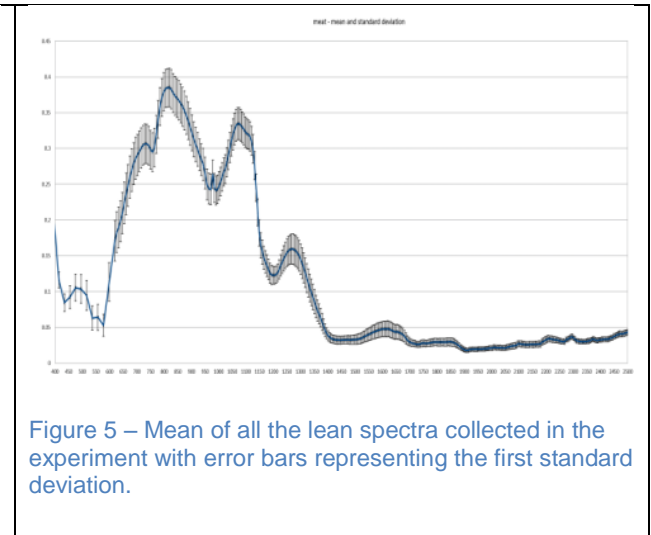


Figure 5 – Mean of all the lean spectra collected in the experiment with error bars representing the first standard deviation.

Although the data appears to be homogeneous, in particular in the infrared wavelengths exceeding 1000nm, it is difficult to understand if the rate of change in spectral intensity is changing. To gain a better understanding of this wavelengths were chosen that represent peaks and drops in the spectra. Gradient between the intensity at each corresponding wavelength was calculated then scaled by a factor of 1000. The graph in Figure 6 is an illustration of the variation in gradient across all 30 samples collected for the experiment.

Using this information, we can establish a threshold for each band ratio combination. This information is another illustration of how homogenous the band ratios are across the 30 samples collected.

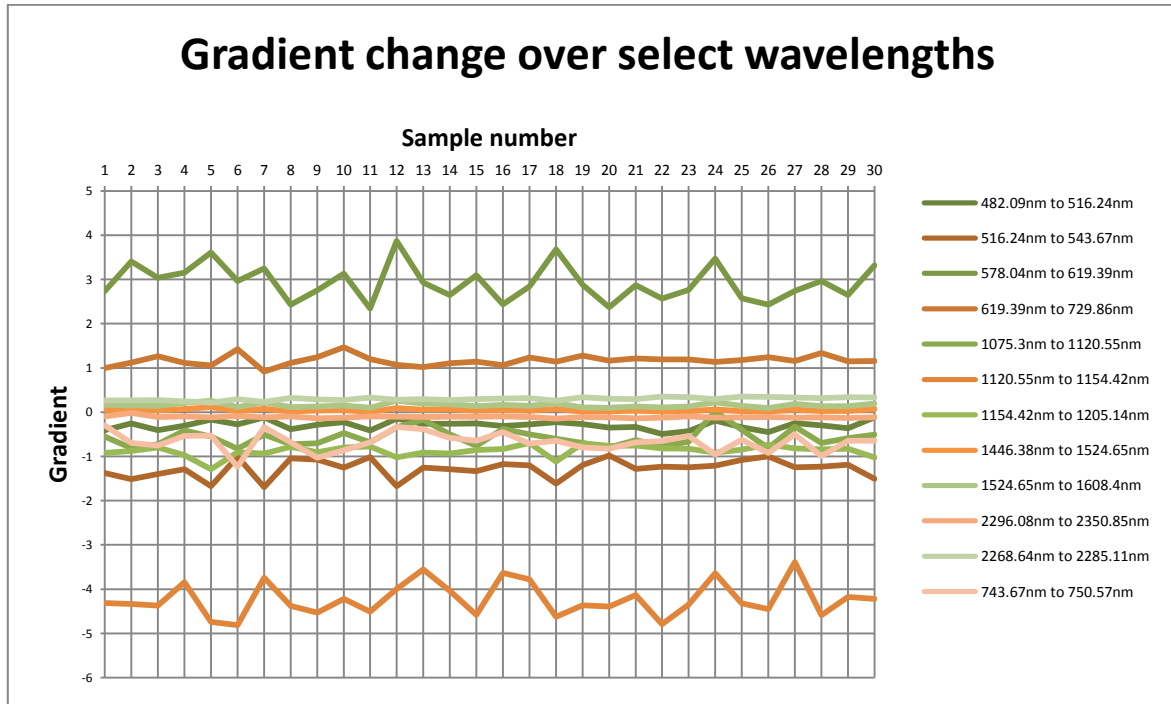


Figure 6 - Chart representing the rate of change in intensity across manually selected wavelengths of light

#### 4.1.3.2 *Fat Spectral Deviation*

Similar to the lean/protein analysis, samples of fat were gathered and analysed together. Observing Figure 7 and Figure 8, it is clearly visible that the spectral deviation in the VNIR (visible to near infrared typically 380nm to 1000nm) part of the spectra shows a significantly larger amount of variation than the lean samples. This is however the opposite when looking at the SWIR (short wavelength Infrared typically 1000nm to 2500nm). This part of the spectra is incredibly homogeneous. The gradient results for fat (Figure 9) indicate a much broader deviation than lean. This is true particularly for wavelengths in the VNIR part of the spectrum.

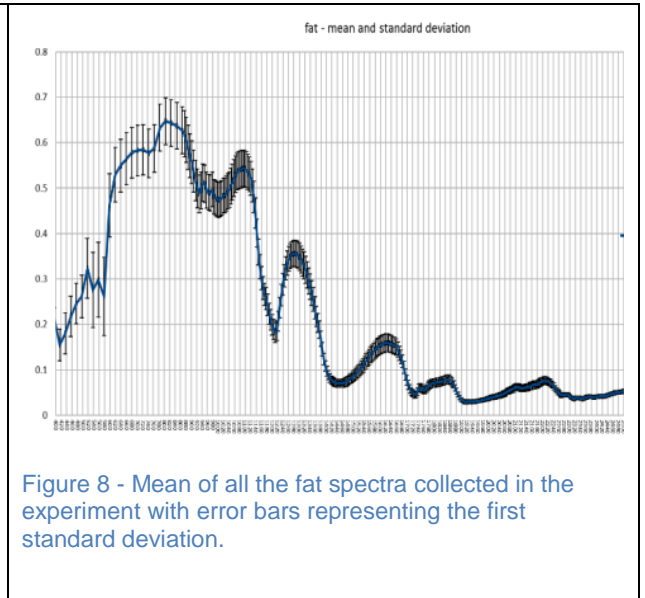
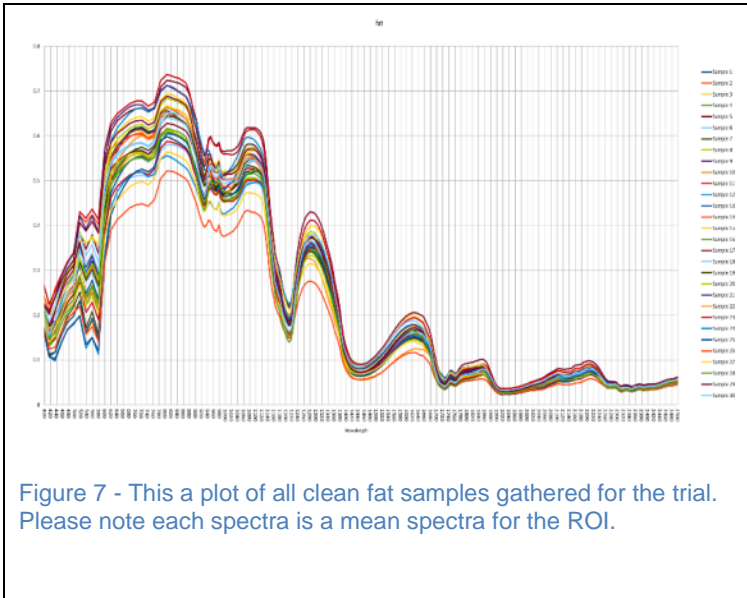


Figure 7 - This a plot of all clean fat samples gathered for the trial. Please note each spectra is a mean spectra for the ROI.

Figure 8 - Mean of all the fat spectra collected in the experiment with error bars representing the first standard deviation.

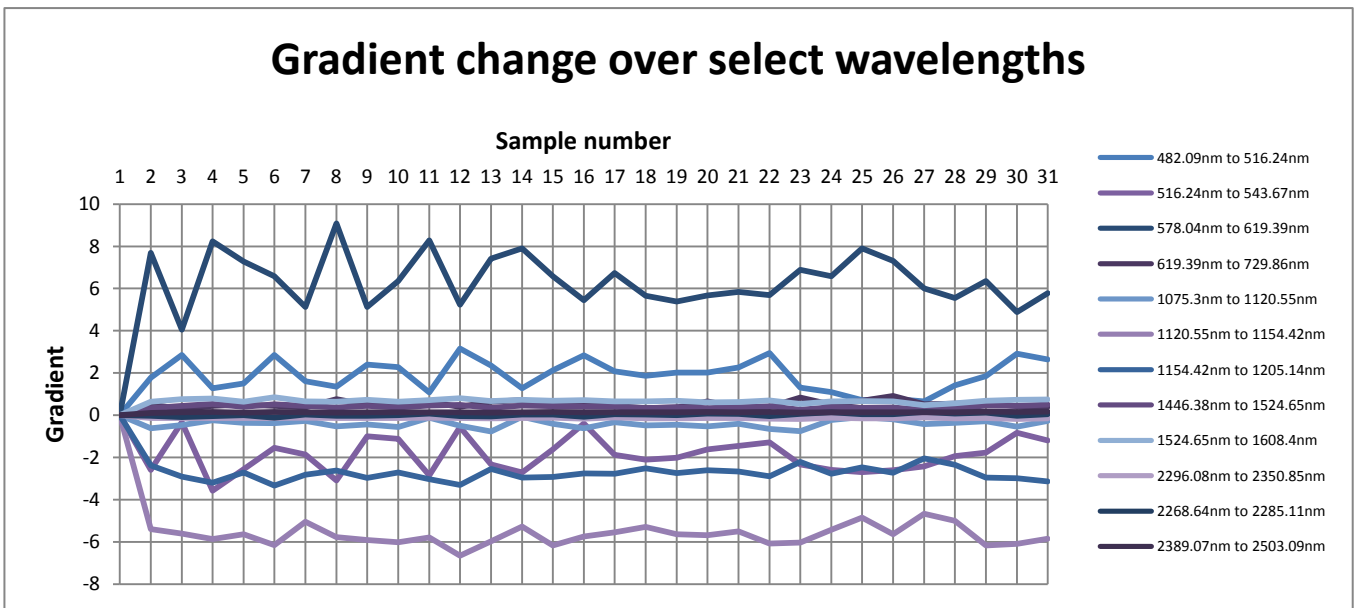


Figure 9 - Gradient deviation results for fat samples.

#### 4.1.4 Conclusion

The results above indicate that fat and lean samples collected from the same area of the carcass, from animals raised the same herd, is relatively homogenous. From these results we are able to pre-empt rough thresholds for rate of change in the intensity of select wavelengths to classify uncontaminated meat and fat. These thresholds were found to be quite stable at certain spectra, despite the natural variation exhibited in the raw spectra across all samples due to the method of analysis utilised. This is an important enabler in the commercial feasibility of the system. Utilising the gradient method of identification also

enables a carcass to become its own control when looking to identify contamination. This is critical due to the natural variation exhibited, not only across carcasses, but potentially within the same carcass across different body areas.

Subtracting the fat spectrum from the meat spectrum indicates that the best wavelength for discrimination between these two tissues should occur at 600nm. This is expected as the red channel in the visible spectrum is the best channel with which to visualise the difference between lean meat (red) and fat (white). If this method is not able to robustly deal with the natural variation experienced, other discriminatory wavelengths can be identified by multivariate analysis of the spectral data. Such methods include principle component analysis (PCA), stepwise discriminant analysis (DA), partial least square-discriminant analysis (PLS-DA), neural networks and genetic algorithms.

Another possible path forward in developing a commercial system may involve building a database of spectra for a range of different tissues (e.g. meat, fat, cartilage, bone etc.) and contaminants. Such a database could be used to bolster analysis.

## **4.2 Trial two – investigating small amounts of contamination**

### **4.2.1 Aim**

One key driver for this project is to identify contaminants that operators on the production floor might otherwise miss. Therefore, it is important to test not only the detection of the contaminants of interest, but also how very small amounts (not visible to the eye) of contamination affects the spectra of clean product.

### **4.2.2 Method**

The following method was used for conducting the experiment:

- The camera exposure and lighting settings were configured so that the maximum intensity of the spectra on the Spectralon plate is at 70 percent of the capability of the camera.
- A white and dark calibration image were acquired.
- Clean samples were prepared from one single cut of beef fat and muscle.
- Where feasible, contamination was coated on the surface of clean fat and meat, making sure to cover the entire surface of the product. This avoided confusion with the uncontaminated surfaces on the sample. Several concentrations of contaminant were tested.
- Samples were sterilised after testing.
- Equipment used for spiking samples was sterilised with alcohol and boiled.
- Equipment that was not in contact with the samples was sterilised with alcohol.
- Each sample was individually analysed.

- A mean spectrum was recorded into a CSV file (approximately 10MB in size, with each raw scan being approximately 300MB in size) with the file name being the timestamp of the original data file for traceability.
- Region of interest for the mean spectrum were selected based on the clearest part of the image with no deep cavities that cast a shadow over the inspection surface.

#### 4.2.3 Results

The comprehensive register containing the trial results for all trials conducted in sections 4.2, 4.3 and 4.4 is shown in Appendix A – Initial trial Results Register. Please take note of the conclusion for each scan.

Initial attempts at identifying unique spectral features for ingesta and faeces visually demonstrated a high degree of confidence that algorithms could be written to identify ingesta and faeces contamination on both muscle and fat surfaces. By tailoring a camera to the relevant spectra and improving spatial resolution, low levels of these contaminants should be detectable in a commercial setting and potentially at a relatively low cost.

Bile was able to be identified in large concentrations once freshly applied to both muscle and fat samples. This ability became diminished after a short period of time, as it's absorbed by the samples. Significant opportunity was still demonstrated and further analysis is being conducted to identify what may improve this result.

Urine was the most challenging contaminant investigated with currently no obvious influence upon the spectra of muscle or fat once applied. This is being further investigated.

Early analysis of contaminant that was diluted indicates that, as long as the portions of the contaminant fits within the bounds of at least one pixel (approximately 0.5mm long in the travel direction by 2mm wide), then the contaminant will be detectable by the camera. Diluting the concentration to subpixel sizes with require the use of complex spectral unmixing algorithms to detect this. Some of this spectral mixing is also caused by motion blur. Please refer to Figure 10, Figure 11 and Figure 12 for an example of the effect of motion blur. In designing a commercial system, the spatial resolution of the camera would first be evaluated to target the particular application. Secondly, the optics would also be optimised. These two design considerations would drastically reduce the effect of these factors.

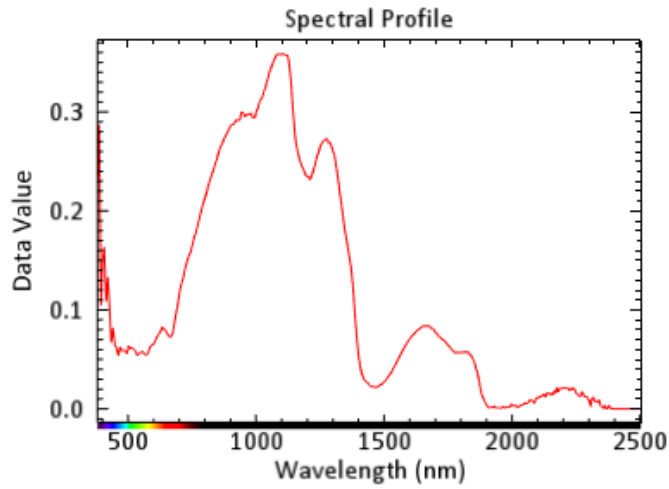


Figure 10 - Spectra of faeces, undistorted by other substances

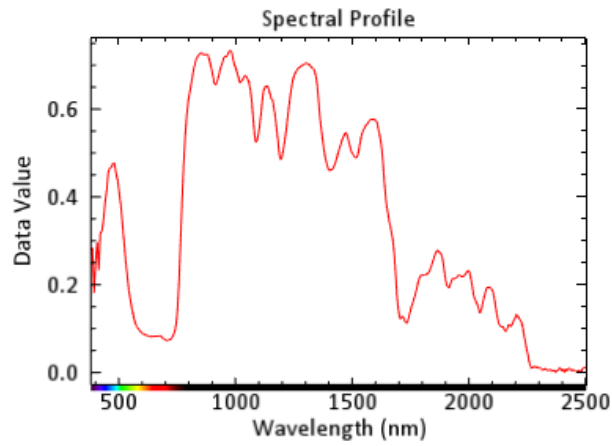


Figure 11 - Spectra of the conveyer on which scanning is performed.

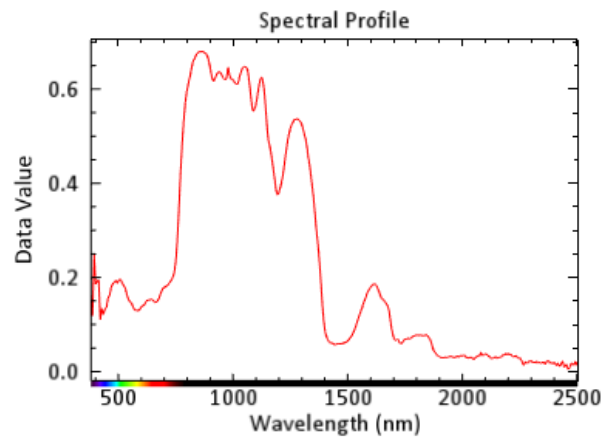


Figure 12 - Spectra of a small portion of faeces on the conveyor, affected by motion blur



## Conclusion

Ingesta and faeces demonstrated a clear ability to be distinguished, even when present on tissue samples. Bile was able to be identified in large concentrations on tissue, but this diminished after a short period of time after which it became absorbed. This suggests potential promise in the application and should be further investigated. Urine presented no immediate discernible change in the spectra for uncontaminated tissue but requires further investigation.

One factor which may affect the spectral features of contamination is ageing in a chiller environment. Depending on where the contamination detection system is located along the processing chain, such a factor may present an opportunity for more robust detection or detection of contaminants which are currently deemed difficult to identify, such as urine and bile.

Having a good knowledge of the base spectra for 'clean' fat and meat may provide a robust solution for contaminant detection in general. In this case, a good database would allow the identification of both specific contaminants, but also non-specific contaminants, by looking for deviations from the norm. Similar methods outlined in section 4.1.4 can be used to identify discriminant wavelengths for specific contaminants with greater detail.

The classification algorithm used for these initial analyses was a *decision tree classifier* which uses a series of binary decisions to separate pixels into classes. It is felt that this method demonstrates significant promise, particularly in the case of faeces and ingesta.

Despite little success being achieved in the initial trials to identify urine and bile, a number of considerations could be applied in a follow-up experiment in an attempt to achieve a successful result. It should be noted that urine and bile detection using hyperspectral is an area without reference in literature at this point in time. First, a larger dataset of contaminated and uncontaminated samples would need to be obtained. The sample for this dataset should cover a wide variety of factors such as breed, gender, diet (particularly grass vs grain fed) and stress level (by using ultimate pH as an indicator). The data can then be analysed using a number of supervised, multivariate methods in order to try and establish a contamination model. This would enable any spectral patterns which exist across multiple wavelengths to be identified.

## 4.3 Trial three – Microbiological contamination

### 4.3.1 Aim

Microbiological contamination is a significant concern in meat processing plants. In particular, *E. coli* is routinely tested for in processing plant around Australia especially for products exported to the USA. *Salmonella* and *Listeria* may also exist in the processing plants and cause contamination issues.

Most healthy ruminant animals have traces of *E. coli* and cross contamination occurs during processing through poor practices or accidental puncture of gut content. *E. coli* are a

diverse and large group of bacteria most are generally harmless to humans. Some *E. coli* known as *Shigatoxigenic Escherichia coli* (STEC) have developed an ability to cause disease in humans.

Sampling and testing remains an inefficient means of controlling microbiological quality. Australia currently collects 60 samples from 12 cartons and tested product can still cause disease. Automating the detection of *E. coli* with the use of a Hyperspectral camera would significantly improve the existing industry practice.

Traditionally *E. coli* is detectable through transmission spectra using a spectroscope. Therefore, it may be detectable using reflectance. We need to identify its effect on the underlying spectra and the limitation in spatial resolution of the camera.

The aim of this experiment was to test the ability of a Hyperspectral camera to detect any form of microbiological contamination of the surface of meat and fat. To have the best chance of success, a very high concentration of *E. coli*, *Salmonella* and *Listeria* was initially used to conduct the experiments.

#### 4.3.2 Method

The same methodology as outlined in section 4.1.2 was used for these trials. Microbiological contaminants were handled by an experienced microbiologist.

#### 4.3.3 Results

The comprehensive register containing the trial results for all trials conducted in sections 4.2, 4.3 and 4.4 is shown in Appendix A – Initial trial Results Register. Please take note of the conclusion for each scan.

The microbiological contaminants (*Salmonella*, *Listeria* and *E. coli*) demonstrated some potential signatures of interest when examined in isolation, even at low concentrations. However, it became difficult to isolate these signatures once the contamination was present on meat tissue. *E. coli* was also tested on a stainless steel surface with similar difficulties. The fact that there were possible signatures visible in isolation demonstrates some potential in still being able to identify these contaminants.

To test the absorption effect of microbiological contamination a small amount of media with a known concentration of contamination was spread in a petri dish. This was then scanned on top of the Spectralon plate. Initial analysis of the mean spectra indicates possible trends in parts of the spectra where clean media have the noticeable absorption differences to contaminated samples.

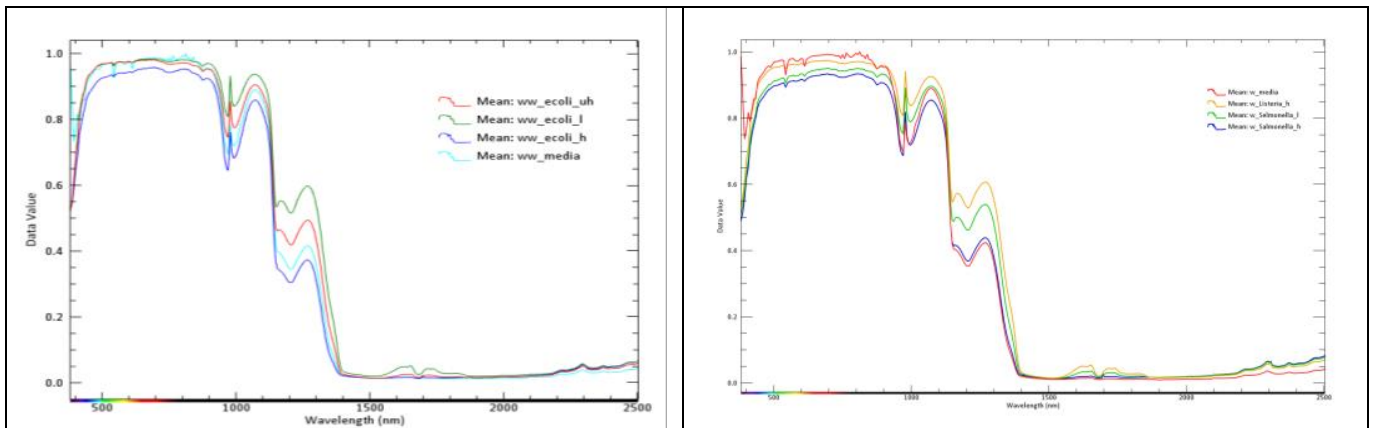


Figure 13 - These are the mean spectra of each of the Micro samples. Note the intensity of the light at 1640nm. Uncontaminated media has the highest absorption of light at this point

When performing the trial, it was difficult to control the volume of each sample due to the way the meniscus was formed. Some of the absorption differences in other parts of the spectra may be explained by this.

Micro contamination on the surface of meat and fat have not yet produced any measurable differences in the spectra but this is being further analysed.

#### 4.3.4 Conclusions

Three microbiological contaminants were investigated – *Salmonella*, *Listeria* and *E. coli*. These demonstrated potential unique signatures when examined in isolation which is an important starting point. It was found that the ability to distinguish these signatures diminished once the contamination was present on lean and fat tissue. The initial result demonstrates promise and further trialling and data analysis is required to investigate this further.

### 4.4 Trial four – effect of UV lighting

#### 4.4.1 Aim

Ultraviolet (UV) lighting is commonly used in the medical and food industries to fluoresce potential contamination on different surfaces. Illuminating a surface with UV light can cause the different substances on the surface to fluoresce different wavelengths of light.

UV lamps are divided into three categories:

- UVA ranges from 400 to 315nm. These wavelengths are not considered dangerous but long exposure can cause skin aging and wrinkles.
- UVB ranges from 315 to 280nm. These wavelengths are considered dangerous - long exposures can cause burns, cataracts and immune system damage.

- UVC ranges from 280 to 100nm. These wavelengths are considered destructive. This wavelength of light is also known as germicidal and is commonly used to disinfect surfaces. They damage the cells' ability to reproduce hence killing the microorganism. The exposure of germicidal ultraviolet is the product of time and intensity. High intensities for a short period and low intensities for a long period are fundamentally equal in lethal action on bacteria.

The main aim of this experiment was to identify how ultraviolet lighting affects the spectra of fat, protein and the range of different contaminants. The test examined the effects of UVA, UVB and UVC wavelengths of light.

#### 4.4.2 Method

Trial two and trial three (sections 4.2 and 4.3, respectively) were conducted using both standard lighting as well as a 95W light with three lamps producing UV A, B and/or C wavelengths of light.

#### 4.4.3 Results

The comprehensive register containing the trial results for all trials conducted in sections 4.2, 4.3 and 4.4 is shown in Appendix A – Initial trial Results Register. Please take note of the conclusion for each scan. It can be seen that, for the trials conducted, UV lighting provided little differentiation when compared to standard lighting.

The challenges of illuminating a surface with UV light is the intensity of the fluorescence emitted from the sample. The usual way of dealing with such problem is changing the optics to allow more light into the cameras sensor. The spectral camera used for the trial has fixed optics therefore the only way around the problem is to increase the exposure of the camera. The unfortunate consequence of a long exposure is motion blur, where the light from the surrounding material can affect the pixel being analysed. What this means is that contamination that has a very small surface area will exhibit spectral characteristics of the surrounding pixels and more than likely be undetectable or at best require a complicated spectral unmixing algorithm to obtain the underlying spectral information.

It is interesting to note that some materials will fluoresce close to 1000nm. Most fluorescence occurs in the infrared wavelength outside the visible range. Substances outside the scope of this trial such as milk and abscesses fluoresce in the visible spectra, exhibiting a yellow colour for milk and a pink colour for abscess. Clean fat tends to fluoresce in a white colour within the visible range. UV lighting thus presents significant opportunity as an enabler for Hyperspectral imaging analysis for contamination detection.

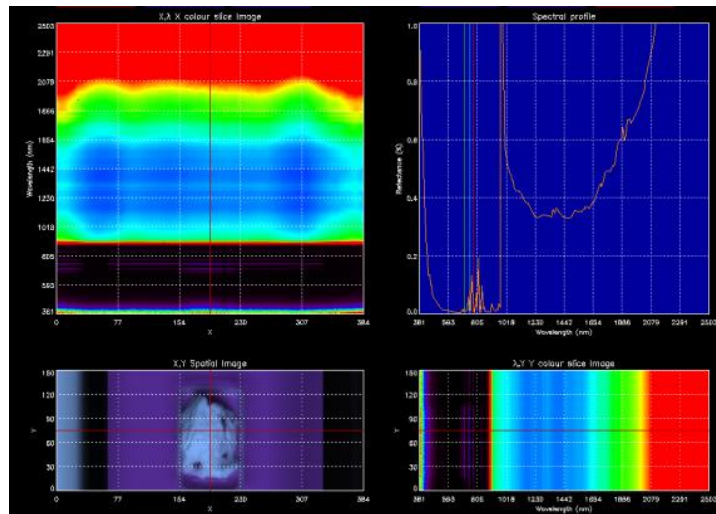


Figure 14 - Screenshot of fat and faeces captured under UV light. Please note the faeces did not fluoresce under selected wavelengths of light. It is also possible to make out slight patterns in the colour slice images that represent the fluorescence of the fat.

#### 4.4.4 Conclusion

The use of UV lighting presents a significant opportunity area for improving the results obtained in the trials with traditional white lighting. This is particularly true for contaminants initially found to be quite challenging (e.g. microbiological contamination, bile and urine). The use of UV lighting presents its own set of challenges however, particularly around the calibration of the camera and the speed with which the camera can be run. The results thus far confirm that UV lighting is a key opportunity area for Hyperspectral imaging technology: by enabling the detection of contaminants not possible with white light; by enabling more robust detection of smaller levels of contamination; and potential for application to other forms of contamination. Some aspects of this will be managed to some extent by the selection of a particular camera hardware for a given application, particularly with respect to spectral range, spectral resolution, spatial resolution and optics.

## **5 Trials Stage 2 – Focused trials (ingesta and faeces)**

At the conclusion of the stage 1 trials it was discovered that there is a significant amount of spectral variation amongst different muscle groups of a single animal. Upon further investigation, it was also discovered that the spectra of meat and fat was relatively homogeneous when looking at a single muscle group across the sample set of animals.

Other trials were also conducted to examine the most reliable algorithm for the detection and classification of the contamination. Decision tree classification was identified as the most reliable algorithm for managing the variation of meat and fat.

Faeces and ingesta were seen to be the most promising contaminants for detection using hyperspectral technology based on initial trialling. They also happen to be the contaminants of highest priority with respect to detection in processing facilities as importing countries also use this as an indicator for good hygiene. It was decided that the next milestone of the project should then focus upon detection of faeces and ingesta. The primary outcome of these trials was to understand the commercial factors and requirements associated with a concept hyperspectral faeces and ingesta contamination system.

### **5.1 Aim**

The aim of this experiment was to dilute the concentration of contaminants and test how well the hyperspectral camera can detect them on the surface of meat and fat. Ultimate success was to be measured by the camera's ability to detect contamination that is invisible to a human eye.

### **5.2 Method**

Ingesta and faeces samples were gathered from the processing floor and the stock yard at a meat processing plant. A Silverside primal with fat covering was purchased from a local butcher.

The following method was used to conduct the experiment:

- The samples were transported to the Tullamarine office for analysis.
- The camera exposure and lighting settings were configured to minimise the effects of spectral mixing and motion blur, while maintaining a good quality spectrum. To achieve this, the individual camera exposure was minimised to a level where the spectral features are still clearly visible, but not necessarily of a high intensity. The camera's scanning frequency was also increased to capture a higher resolution image in the direction of the conveyer.



Figure 15 - Camera exposure and frame rate settings.

- A white and dark calibration image was acquired.

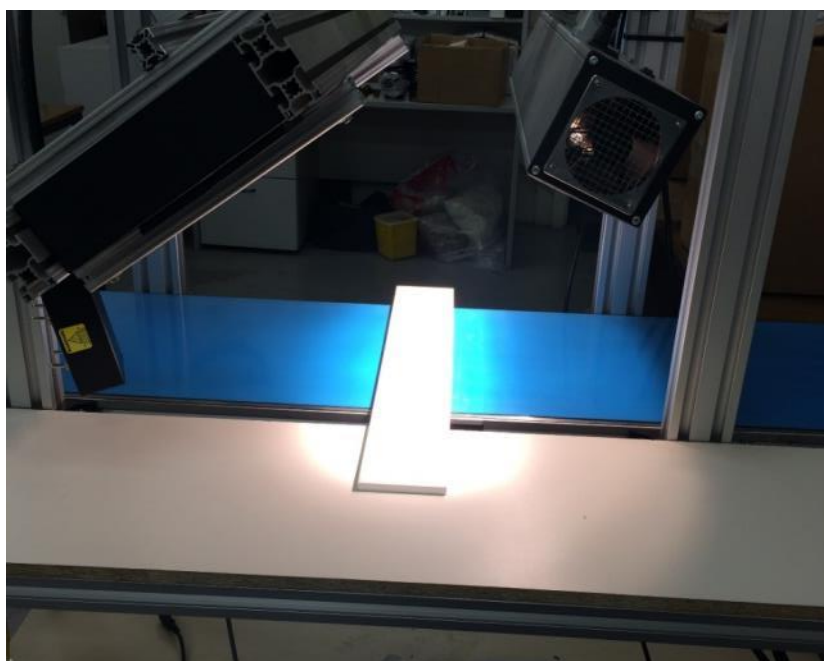


Figure 16 - Calibration process with the Spectralon plate in the cameras field of view.

- Meat samples were cut up into similar sized portions. Half of the fat was then removed from the top of the meat to expose the meat below.



Figure 17 - Preparation of the Meat samples. Please note that the samples were of a similar size.

- Each contaminant was scanned in the undiluted form to better understand the spectral variation of the contaminants.
- The contaminants were then diluted into different concentrations using distilled water.
- Each meat sample was weighed and measured before being scanned.



Figure 18 - Measurement process of the Meat samples.

- A control scan was taken before contaminant was added to the surface of the meat.
- To add contaminant to the surface of the meat, the sample was dipped into the diluted contaminant and excess contaminant was then scraped off. The sample was then reweighed and the weight increase was recorded.
- Each data cube was saved with a timestamp.
- Samples were discarded and equipment sterilised with alcohol.
- Each sample was individually analysed.



Table 1 - Control and contaminated beef samples with different concentrations of faeces

















Control Samples	Samples contaminated with faeces	Contamination Concentration
		<p>12.5%</p>
		<p>25%</p>
		<p>50%</p>
		<p>100%</p>

Table 2 - Control and contaminated beef samples with different concentrations of ingesta

Control Samples	Samples contaminated with ingesta	Contamination Concentration
		12.5%
		25%
		50%
		100%

It can be seen that, while there are significant areas on the meat with contamination visible to the eye, there are also portions where contamination isn't visible.

## 5.3 Results

The following section outlines the trial results.

### 5.3.1 Contaminant spectra

First, the spectra for faeces and ingesta were analysed in order to understand their spectral properties.

#### 5.3.1.1 *Faeces spectra*

For this trial, three different faeces samples were gathered from 3 different animals in the stock yard of the abattoir. Mean spectra of each was collected to work out the spectral deviation and assess any changes in spectra (which could be caused by a number of factors such as breed, diet etc.).



Figure 19 - Faeces samples from 3 different animals. Please note that partially digested material is visible.

Each sample was scanned individually and statistical analysis was carried out on each sample.

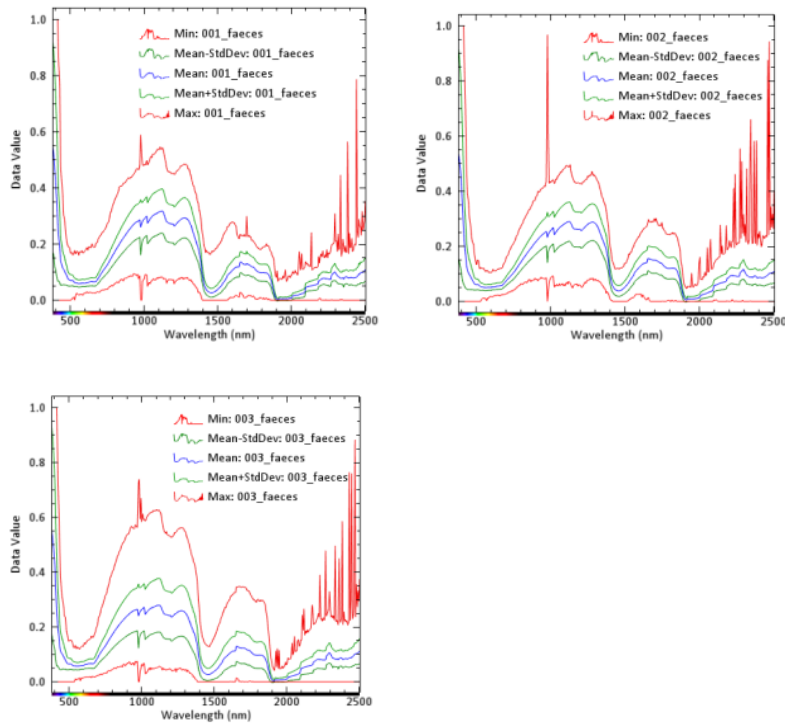


Figure 20 - Graphs of the statistical analysis of each sample.

The analysis carried out in Figure 20 indicates that the spectra of faeces is very constant with the standard deviation being quite close to the mean spectra. There are however indications of 100% light absorption in the minimum spectra, this could have been caused by shadows of the geometry of the object.

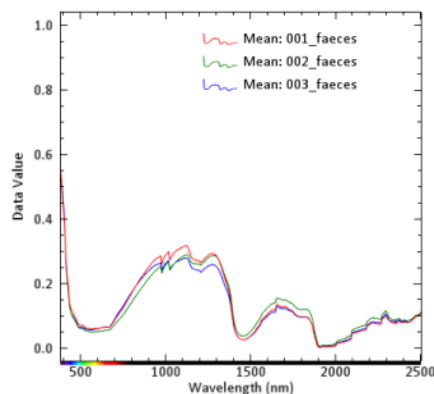


Figure 21 - Mean spectra of all 3 faeces samples.

The graph in Figure 21 indicated that all 3 faeces samples are almost identical spectrally.



### 5.3.1.2 *Ingesta spectra*

The ingesta samples were collected from 3 different animals on the kill floor. Mean spectra of each was collected to work out the spectral deviation.

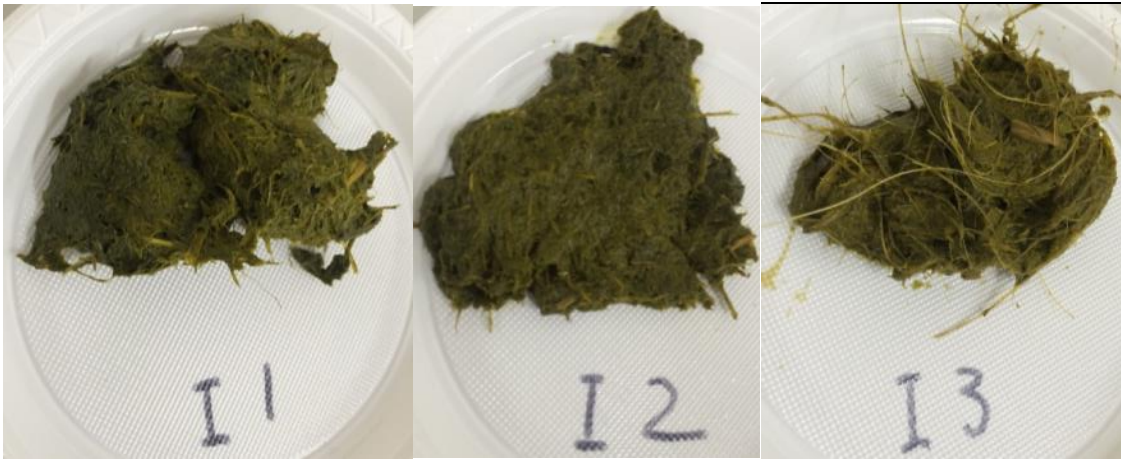


Figure 22 - Ingesta samples from 3 different animals.

Each sample was scanned individually and statistical analysis was performed.

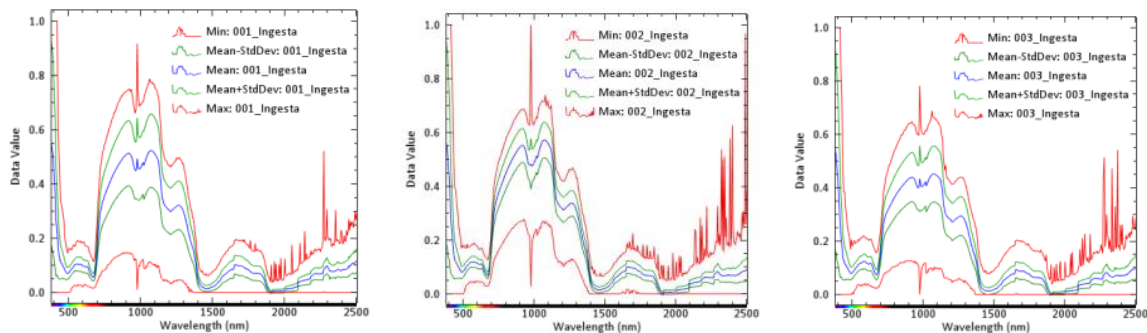


Figure 23 - Graphs of the statistical analysis of each sample.

The analysis carried out in Figure 23 indicates that the spectra of ingesta is very constant with the standard deviation being quite close to the mean spectra. While this is true for the samples analysed, a larger sample will need to be evaluated moving forward to assess with more detail the effect of factors such as breed, diet etc. There are however indications of 100% light absorption in the minimum spectra. This could have been caused by shadows of the geometry of the object. Please note that the maximum spectral deviation of ingesta is closer to the mean than in the faeces samples.

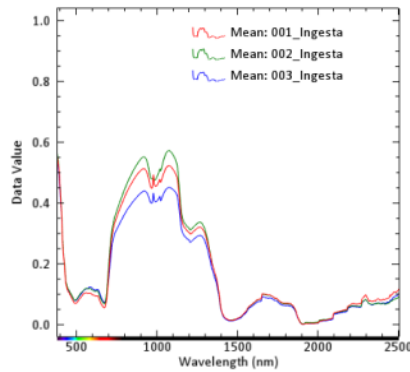


Figure 24 - Mean spectra of all 3 Ingesta samples.

All the samples were very similar in intensity with the exception of 700 to 1000nm exhibiting minor intensity differences.

### 5.3.1.3 **Combination**

Spectra was also gathered of the control samples of meat and fat. The spectra of the contaminants were rendered with the spectra of meat and fat.

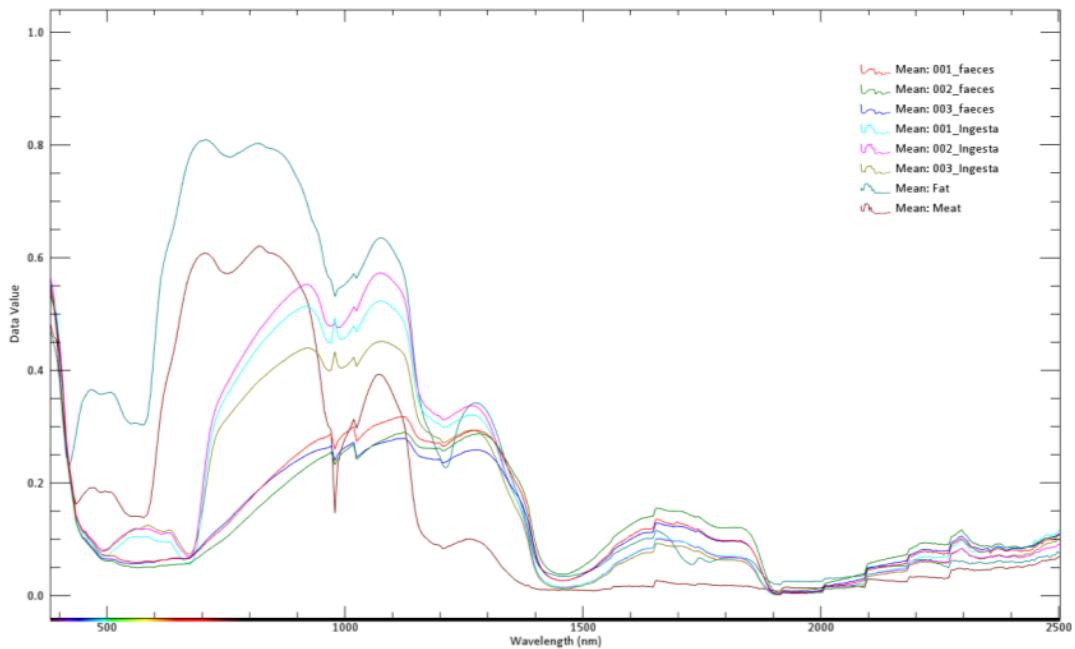



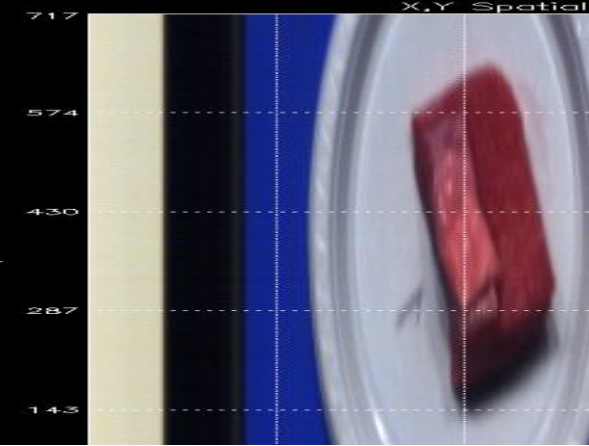
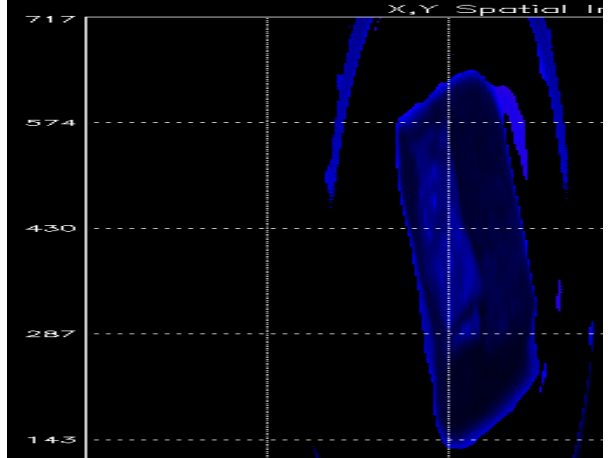

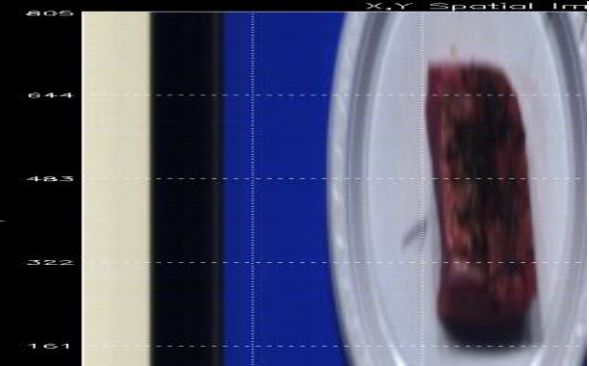
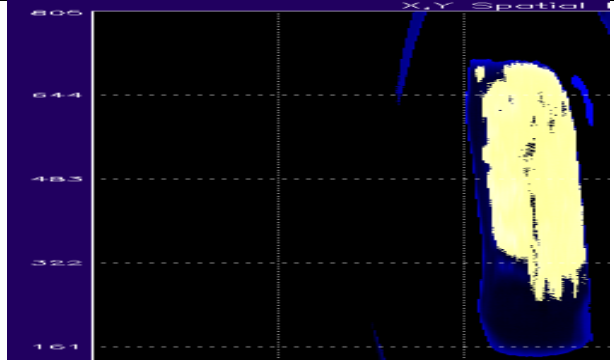
Figure 25 - The Spectral of the contaminants as well as the meat and fat.

From the spectra illustrated in Figure 25 it is clearly obvious that the spectra of meat and fat differs significantly in the visible and infrared portions of the spectrum. Faeces and ingesta also exhibited a sharp increase in spectral gradient between 700 and 900nm. This is a spectral feature knows as the “red peak” and it is a characteristic of chlorophyll.

5.3.2 Diluted contaminants

All samples were scanned and processed using the decision tree algorithm developed the previous milestones of this project.

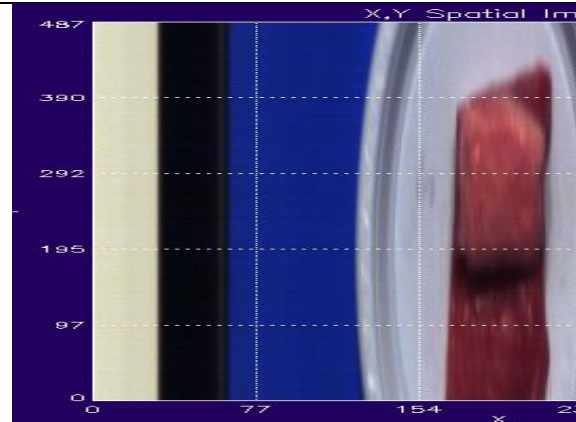
5.3.2.1 *Sample 1 faeces with 100% contamination*

 <p>Photo of the control samples. Dimensions = 55mm x 70mm Weight = 98g</p>	 <p>False colour image of the scanned sample.</p>	 <p>Image of the processed result. Blue colour indicates presence of clean material.</p>
 <p>Photo of the contaminant applied to the same sample. Weight = 99g</p>	 <p>False colour image of the scanned sample.</p>	 <p>Image of the processed result. Blue colour indicates presence of clean material; yellow indicates the presence of contamination.</p>

5.3.2.2 *Sample 2 faeces with 50% contamination dilution*



Photo of the control samples.  
Dimensions = 60mm x 70mm  
Weight = 91g



False colour image of the scanned sample.

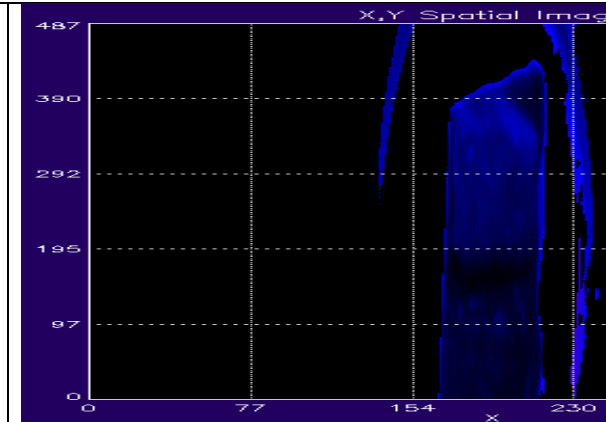
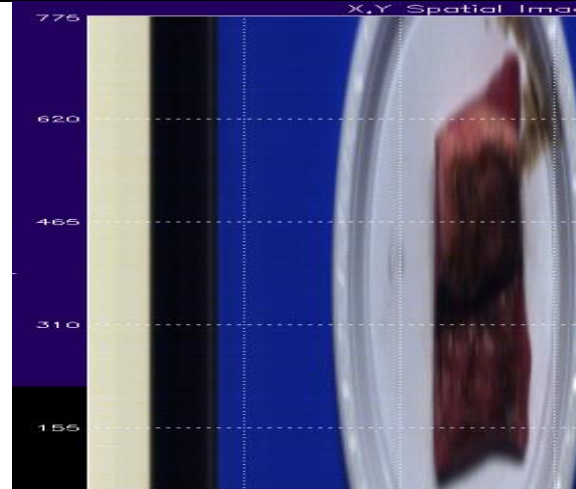


Image of the processed result. Blue colour indicates presence of clean material.



Photo of the contaminant applied to the same sample.  
Weight = 93g



False colour image of the scanned sample.

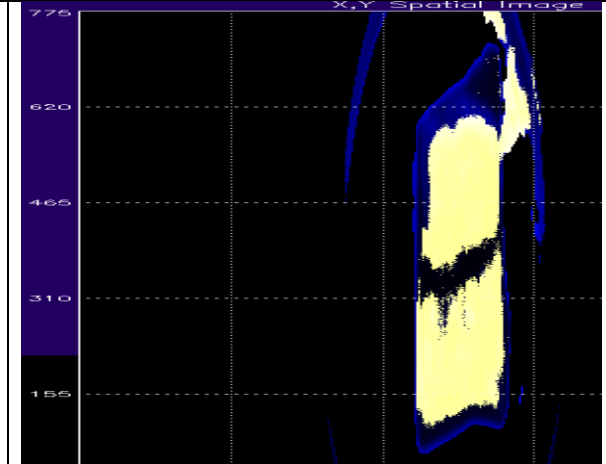

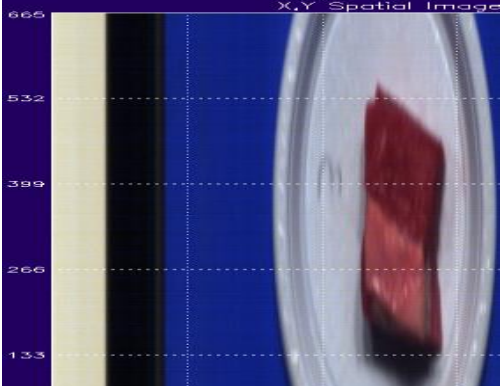
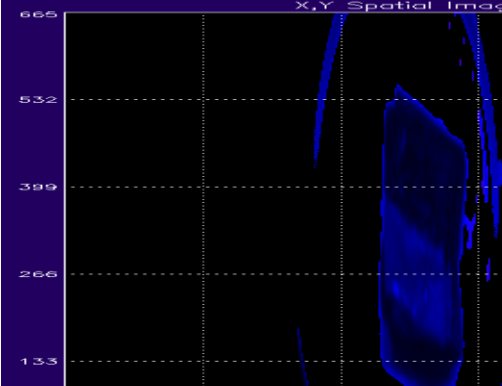

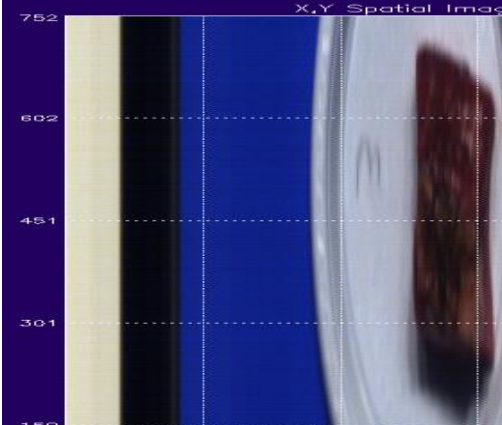
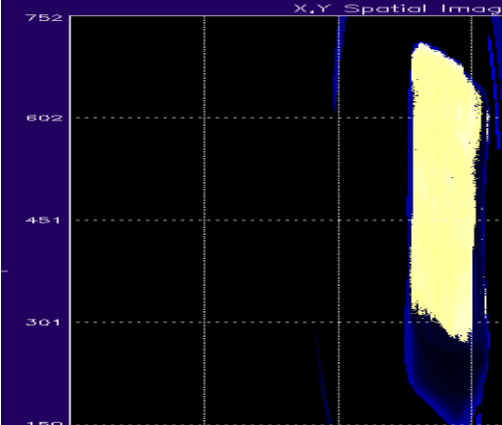



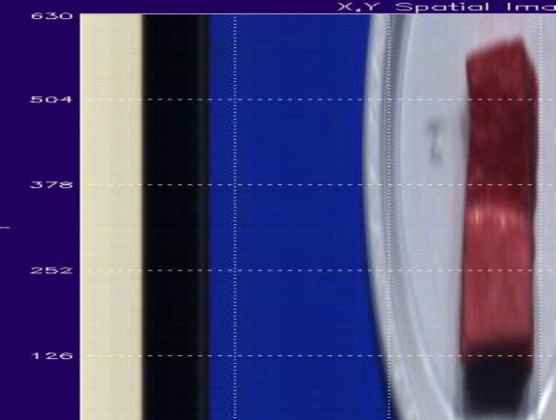
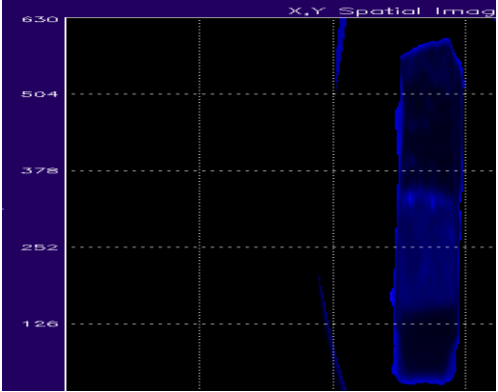

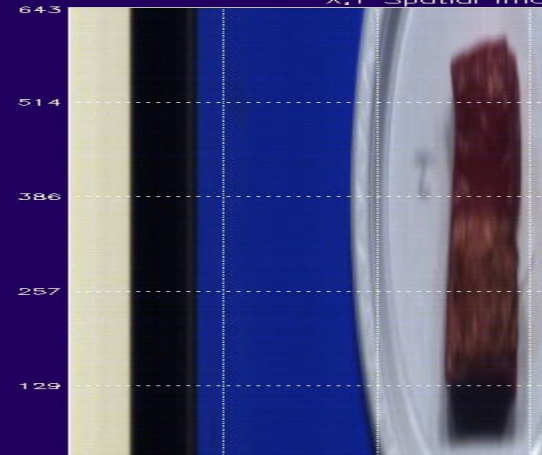
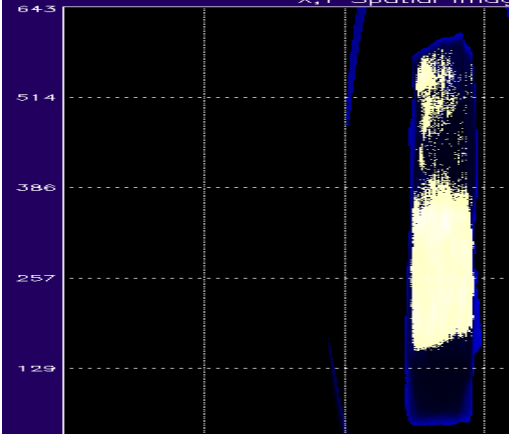
Image of the processed result. Blue colour indicates presence of clean material; yellow indicates the presence of contamination.




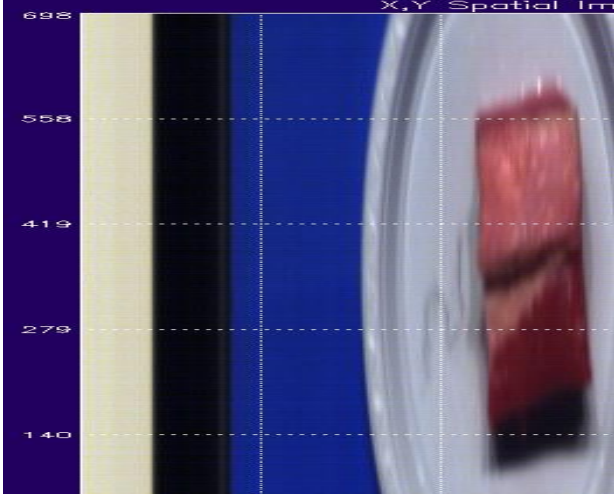
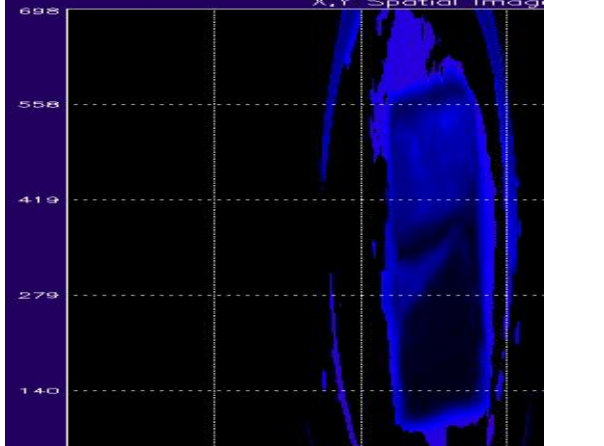

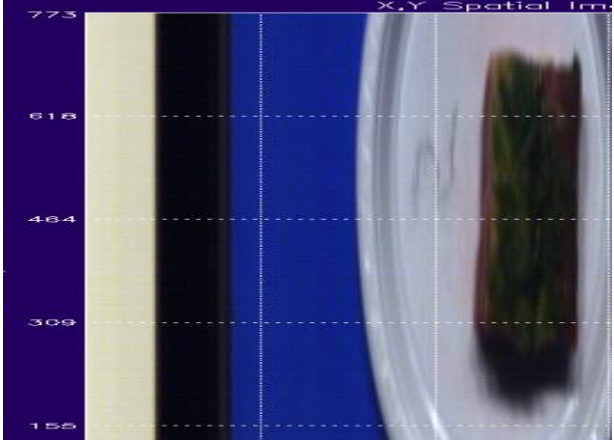
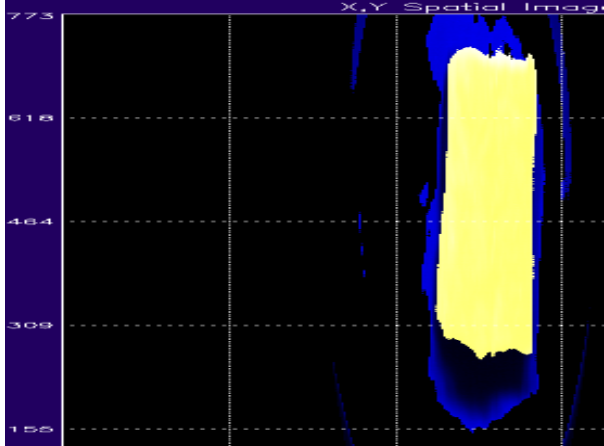
5.3.2.3 *Sample 3 faeces with 25% contamination dilution*

		
<p>Photo of the control samples. Dimensions = 60mm x 55mm Weight = 112g</p>	<p>False colour image of the scanned sample.</p>	<p>Image of the processed result. Blue colour indicates presence of clean material.</p>
		
<p>Photo of the contaminant applied to the same sample. Weight = 113g</p>	<p>False colour image of the scanned sample.</p>	<p>Image of the processed result. Blue colour indicates presence of clean material; yellow indicates the presence of contamination.</p>

5.3.2.4 **Sample 4 faeces with 12.5% contamination dilution**


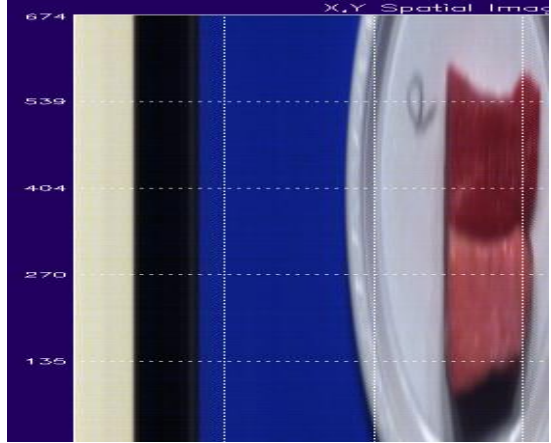
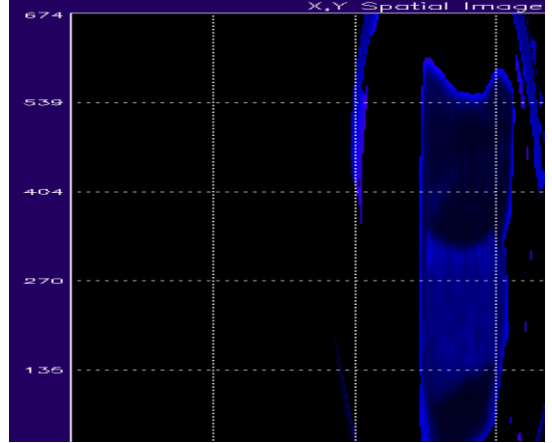

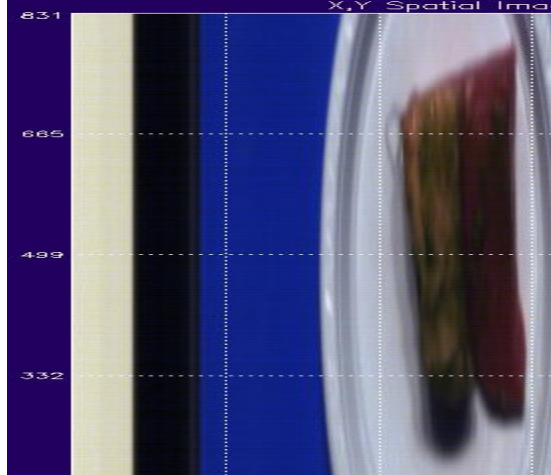
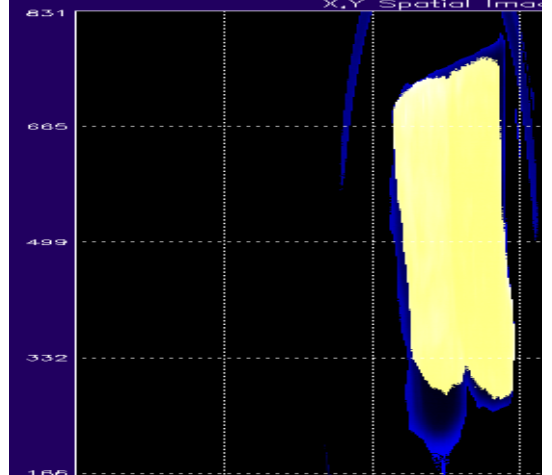
 <p>Photo of the control samples. Dimensions = 70mm x 45mm Weight = 102g</p>	 <p>False colour image of the scanned sample.</p>	 <p>Image of the processed result. Blue colour indicates presence of clean material.</p>
 <p>Photo of the contaminant applied to the same sample. Weight = 103g</p>	 <p>False colour image of the scanned sample.</p>	 <p>Image of the processed result. Blue colour indicates presence of clean material; yellow indicates the presence of contamination. This indicates that, while the contamination is detectable, some improvement to the algorithm is required for detection across the whole surface.</p>

5.3.2.5 *Sample 5 ingesta with 100% contamination*

 <p>Photo of the control samples. Dimensions = 60mm x 55mm Weight = 107g</p>	 <p>False colour image of the scanned sample.</p>	 <p>Image of the processed result. Blue colour indicates presence of clean material.</p>
 <p>Photo of the contaminant applied to the same sample. Weight = 108g</p>	 <p>False colour image of the scanned sample.</p>	 <p>Image of the processed result. Blue colour indicates presence of clean material; yellow indicates the presence of contamination.</p>



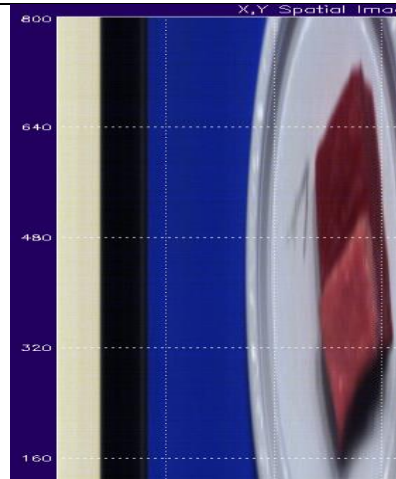
5.3.2.6 *Sample 6 ingesta with 50% contamination dilution*

 <p>Photo of the control samples. Dimensions = 60mm x 70mm Weight = 114g</p>	 <p>False colour image of the scanned sample.</p>	 <p>Image of the processed result. Blue colour indicates presence of clean material.</p>
 <p>Photo of the contaminant applied to the same sample. Weight = 115g</p>	 <p>False colour image of the scanned sample.</p>	 <p>Image of the processed result. Blue colour indicates presence of clean material; yellow indicates the presence of contamination.</p>

5.3.2.7 *Sample 7 ingesta with 25% contamination dilution*



Photo of the control samples.  
Dimensions = 50mm x 70mm  
Weight = 114g



False colour image of the scanned sample.

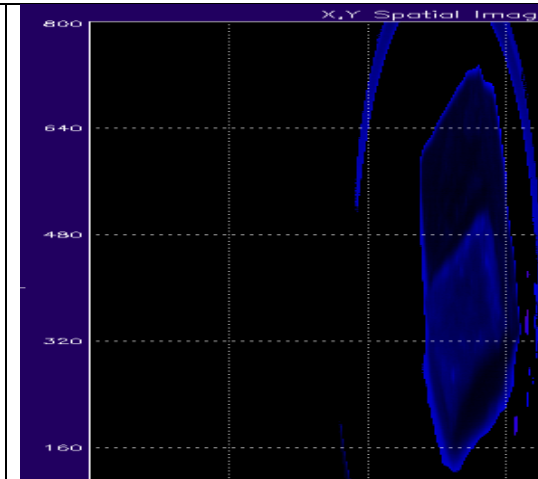
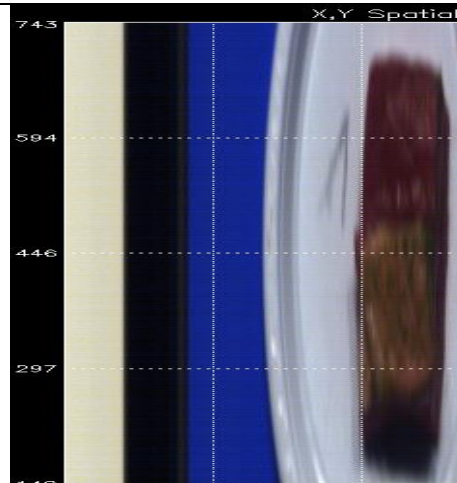


Image of the processed result. Blue colour indicates presence of clean material.



Photo of the contaminant applied to the same sample.  
Weight = 115g



False colour image of the scanned sample.

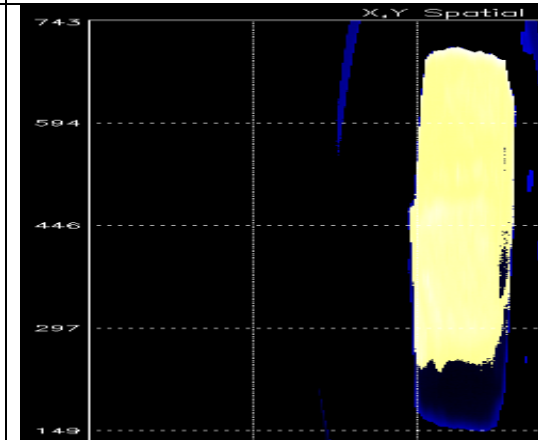
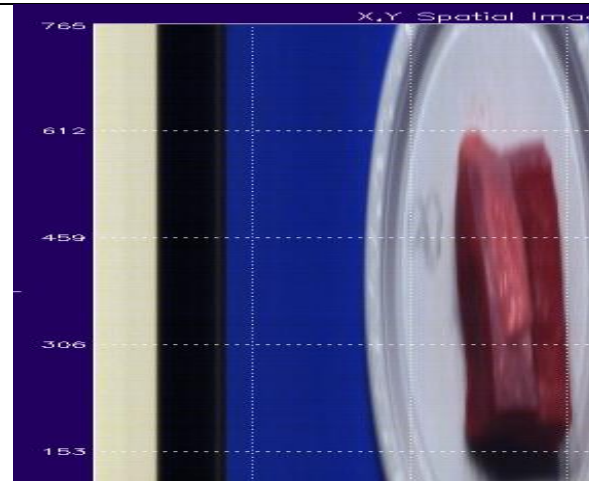


Image of the processed result. Blue colour indicates presence of clean material; yellow indicates the presence of contamination.

5.3.2.8 *Sample 8 ingesta with 12.5% contamination dilution*



Photo of the control samples.  
Dimensions = 50mm x 70mm  
Weight = 144g



False colour image of the scanned sample.

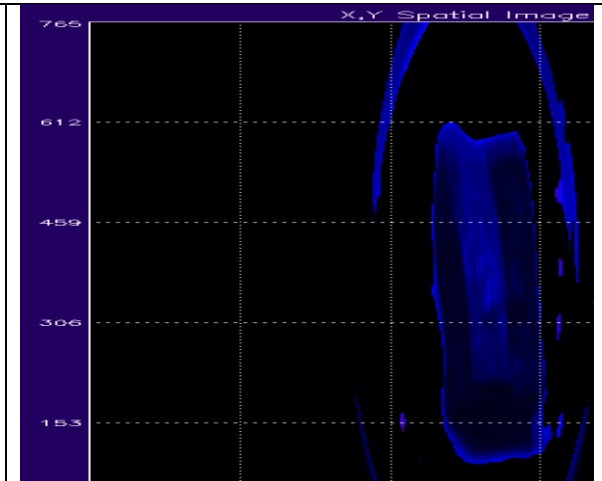
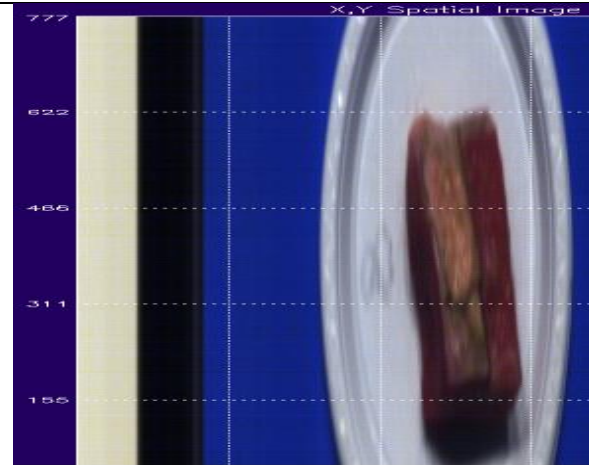


Image of the processed result. Blue colour indicates presence of clean material.



Photo of the contaminant applied to the same sample.  
Weight = 145g



False colour image of the scanned sample.

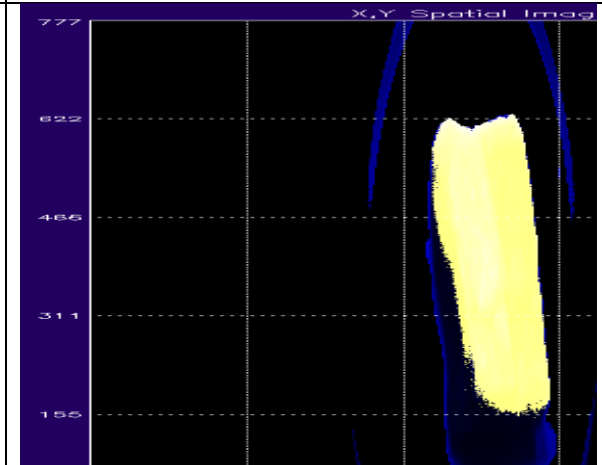


Image of the processed result. Blue colour indicates presence of clean material; yellow indicates the presence of contamination.

### 5.3.3 Conclusions

The results of the diluted contamination trials have proven to be positive. There was no false classification of contamination observed of the control samples during the trial. Contamination was detected on surfaces that had diluted contaminant applied to them that resulted in very little to no visible change. On the meat surface in section 5.3.2.4 (Sample 4 faeces with 12.5% contamination dilution) most of the contaminated surface was detected but there were areas in which the contamination was not accurately flagged (as indicated by the yellow highlighted area being quite patchy on the meat portion of the processed sample image in 5.3.2.4). This suggests that this algorithm would require further tuning to be able to identify faeces contamination on meat at very high levels of dilution.

## 5.4 Secondary Analysis

The faeces and ingesta data was analysed using a second analysis methodology as described below. This allowed further confidence to be demonstrated in the ability to develop a faeces and ingesta detection system using hyperspectral imaging technology.

### 5.4.1 Ingesta

Main spectral data (400-2500 nm) were extracted from all samples using regions of interest (ROIs) centred at fat, lean and contaminated surfaces. This data set consisted of 66 spectra (12 fat spectra, 12 lean spectra and 42 ingesta spectra). Ingesta spectra means that fat or lean portions contaminated with ingesta as well as pure ingesta. Data were then subjected to various multivariate analysis methods. Principal component analysis was first performed to see the general trend of the spectra and to discover whether it is possible to discriminate among these three classes (fat, lean and contaminated surfaces) or not. The results were very promising and revealed that it is possible to distinguish these classes as shown in Figure 26.

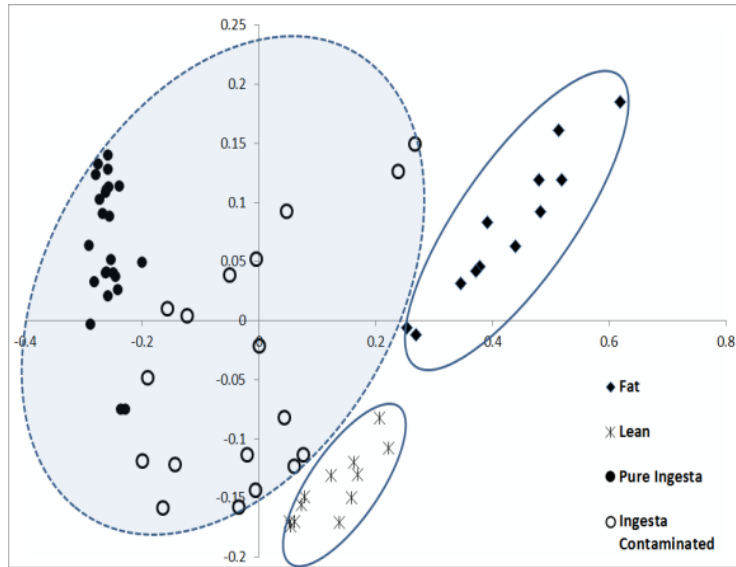


Figure 26 - PCA result for ingesta (mean spectra)

Four wavelengths were then selected and used to build a decision tree classifier. The results of this classification are shown in Table 3. Despite the very high performance of this model in assigning the identity of the mean spectra and identify whether it contains contaminations or not, when this model was used to predict the class of every single pixel in the image the results were less robust. This could be attributed to the fact that the mean spectra do show the real spectral signatures of all pixels (thousands of pixels) in the image. Also, only 66 spectra could be a small number to build a robust model.

Note, this kind of table is referred to as a ‘confusion matrix’. The rows indicate which type of material each sample (in this case, each pixel) is and the columns indicate what it was identified as. Ideally each sample is correctly identified as the correct type. This matrix demonstrates how often that occurs and, in the event of misclassification, which classes are more prone to be misclassified. Some situations are more desirable (e.g. misclassifying ‘clean’ fat or lean as ingesta) over others (e.g. misclassifying ingesta as ‘clean’ fat or lean) although the target is to minimise all misclassifications as much as possible.

Table 3 - Classifier result for ingesta (mean spectra)

from \ to	Fat	Lean	Ingesta	Total	% correct
Fat	11	1	0	12	91.67%
Lean	0	12	0	12	100.00%
Ingesta	0	2	40	42	95.24%
Total	11	15	40	66	95.45%

Instead of extracting mean spectra from each sample (using regions of interest 'ROIs'), a number of spectra were extracted from hundreds of pixels representing the three classes (fat, lean and ingesta contaminated surfaces). This dataset consisted of 2425 spectra (563 fat spectra, 629 lean spectra and 1233 ingesta spectra) collected from samples (control and



contaminated samples). Ingesta spectra means that spectral data were collected from fat or lean contaminated with ingesta in addition to pure ingesta. Data were subjected to various multivariate analysis methods. Principal component analysis was first performed to see the general trend of the spectra and to discover whether it is possible to discriminate among these three classes (fat, lean and contaminated surfaces) or not. The results revealed that it is possible to distinguish these classes as shown in Figure 27.

Due to multicollinearity among wavelength variables, the classification could be improved if only key wavelengths were selected. The classification accuracy was improved when only 9 wavelengths out of 362 wavelengths were used as shown in Figure 28.

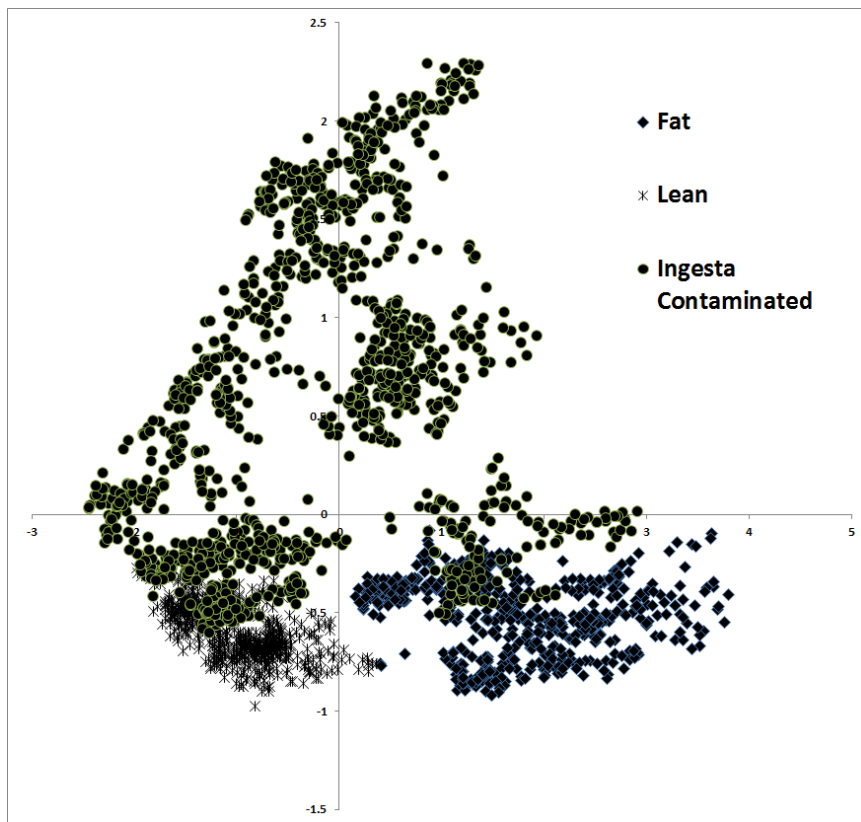


Figure 27 - PCA analysis for ingesta (pixel spectra)

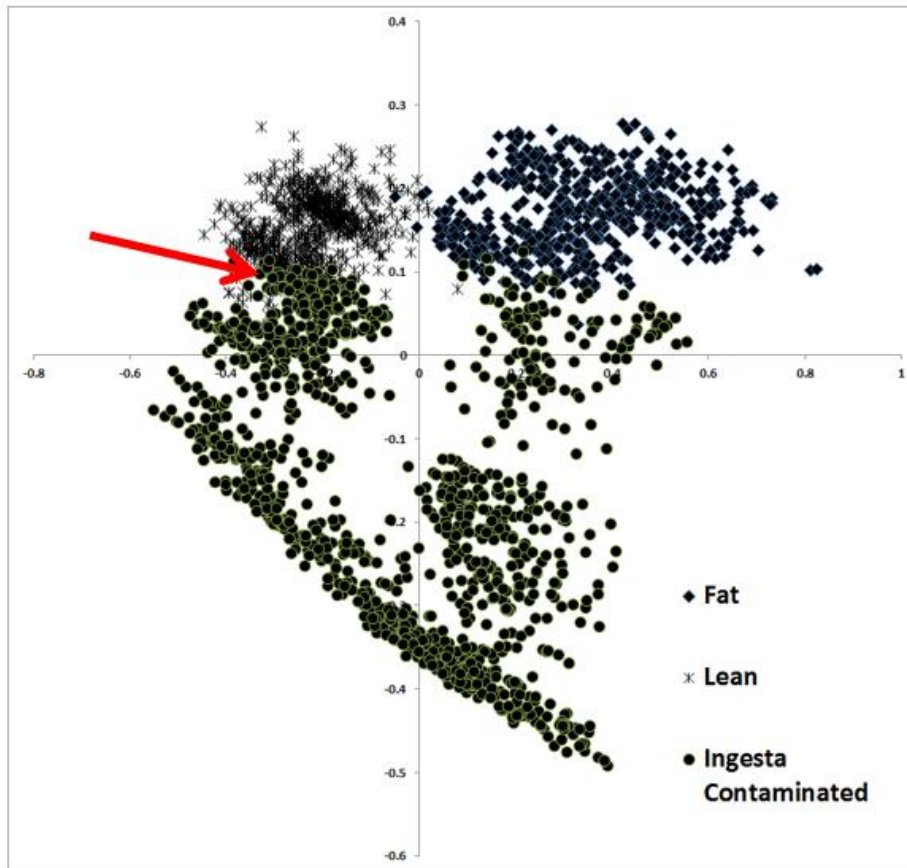


Figure 28 - PCA analysis for ingesta (using key wavelengths)

There are interactions between the lean or fat spectra with those surfaces contaminated with low concentrations of ingesta (12.5%) as the red arrow indicated in Figure 28. Because of this, the key wavelengths were then used in building a new multivariate calibration model not only to classify the spectra but also to predict the identity of every single pixel in the image. For classification of the 2425 spectra under cross validation process, the classification accuracy reached 99.38 % as shown in Table 4. All fat pixels (first class) were accurately classified without any error (100%). The lean meat pixels were also precisely classified with an accuracy of 99.21% but with only five lean meat pixels (the second class) classified as fat pixels. However, based on our assumption, this is not a problem because both surfaces are normal and this misclassification is acceptable as long as these pixels are not misclassified as contaminated class.

Table 4 - Ingesta classification result (pixel spectra)

<b>from \ to</b>	<b>Fat</b>	<b>Lean</b>	<b>Ingesta</b>	<b>Total</b>	<b>% correct</b>
<b>Fat</b>	<b>563</b>	<b>0</b>	<b>0</b>	<b>563</b>	<b>100.00%</b>
<b>Lean</b>	<b>5</b>	<b>624</b>	<b>0</b>	<b>629</b>	<b>99.21%</b>
<b>Ingesta</b>	<b>0</b>	<b>10</b>	<b>1223</b>	<b>1233</b>	<b>99.19%</b>
<b>Total</b>	<b>568</b>	<b>634</b>	<b>1223</b>	<b>2425</b>	<b>99.38%</b>

For the classification of the images, the same model was applied in all images provided and the following outcomes were obtained (Figure 29). It could be clearly noticed that the model was robust and had a high accuracy in detecting contaminated pixels in spite of the original concentrations of the contaminants. The pixels appeared in blue colour in the final classification images means that these pixels are contaminated with ingesta. The misclassification between fat and lean (red and blue colours, respectively) is acceptable according to the assumption we assumed at the beginning because the main aim was to distinguish contaminated portions. By following this protocol, a multispectral system could be designed and fabricated leading to a full automation of the operation (detecting without the presence of any operator).

The model was then analysed for further improvement. Eleven key wavelengths were identified as well as two band ratios to give 13 discriminator variables in total. A new discriminant analysis was then developed. The results (Table 5) demonstrate a significant improvement in accuracy, particularly in the 100% classification rate of contaminated pixels. The overall accuracy of the model is 99.67%, noting that misclassification between uncontaminated fat and uncontaminated lean is of little consequence, as both cases are still uncontaminated tissues. Again, this model was applied to every single pixel in each image, with the results shown in Figure 30.

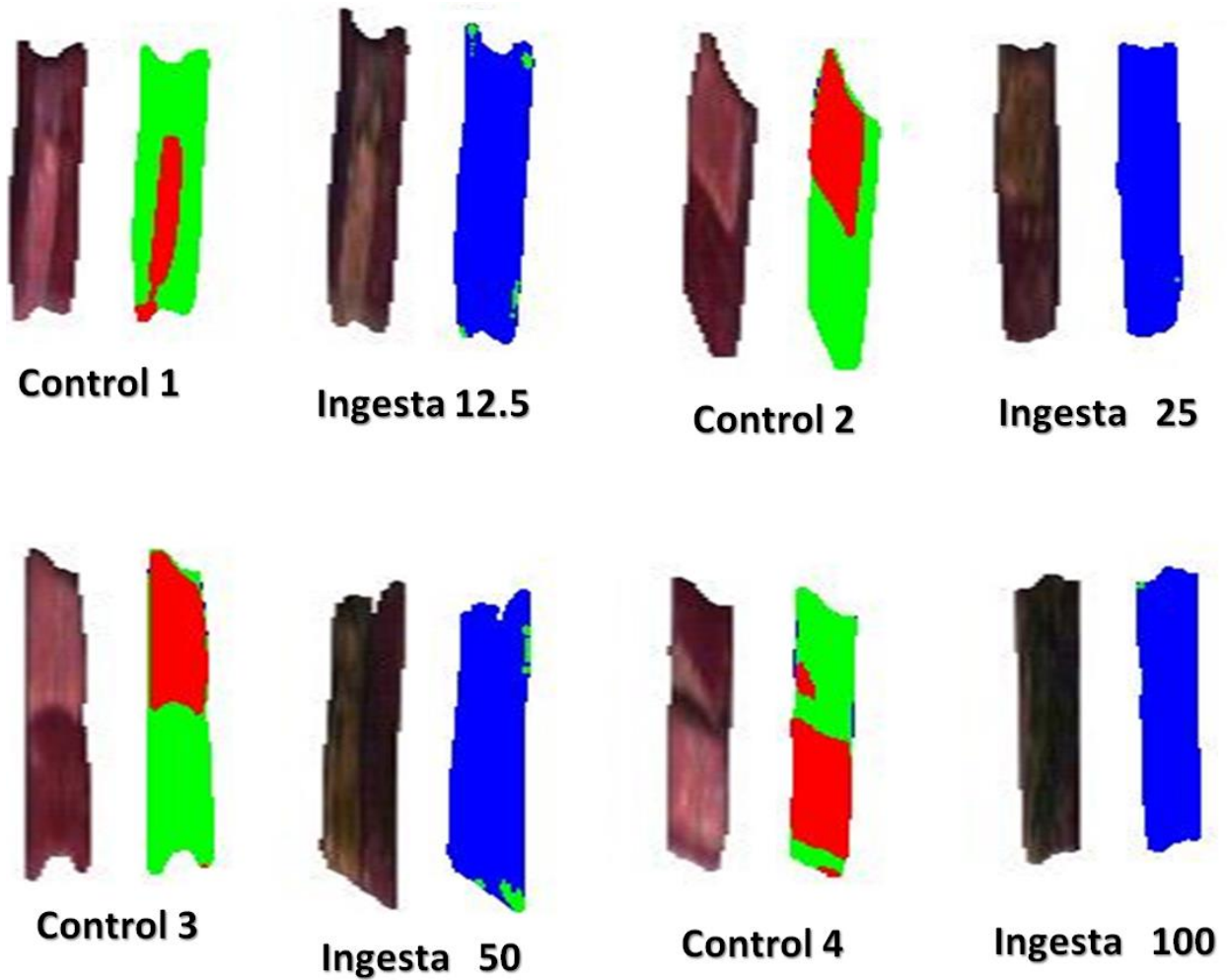


Figure 29 - Classification images of control and contaminated beef samples. Blue indicates contamination with ingesta

Table 5 - Ingesta classification result (pixel spectra) – 11 key wavelengths

from \ to	Fat	Lean	Ingesta	Total	% correct
Fat	563	0	0	563	100.00%
Lean	8	621	0	629	98.73%
Ingesta	0	0	1233	1233	100.00%
Total	571	621	1233	2425	99.67%

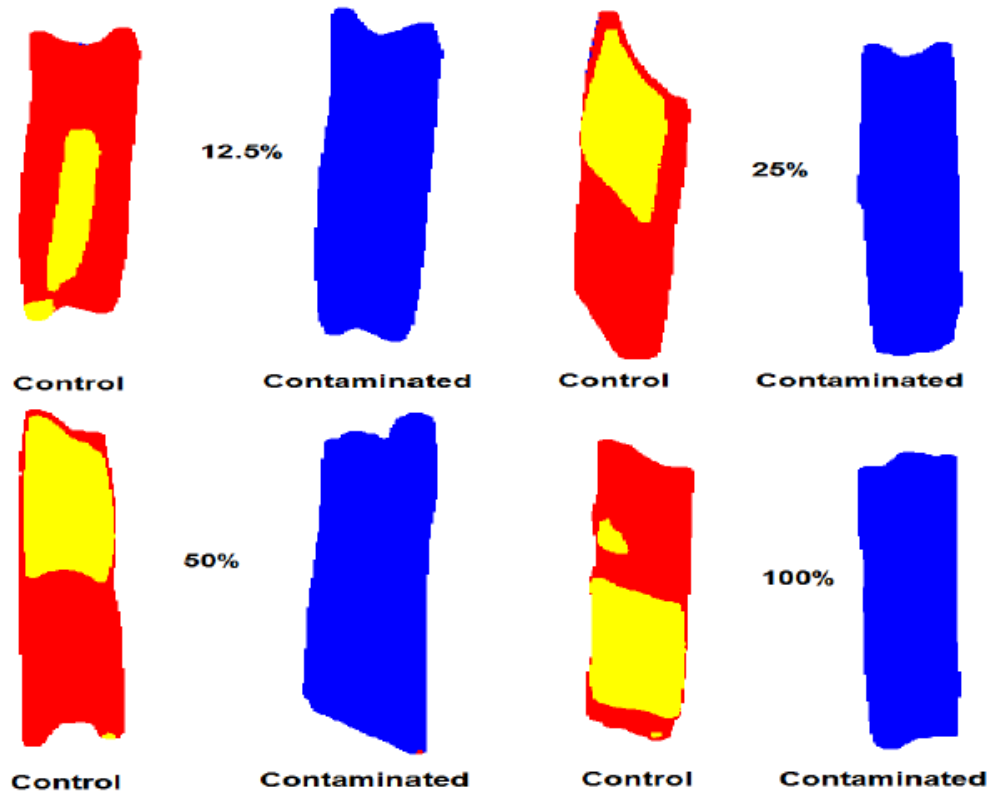


Figure 30 - Classification images of control and contaminated beef samples. Blue indicates contamination with ingesta, Red indicates uncontaminated lean meat, Yellow indicates uncontaminated fat.

#### 5.4.2 Faeces

Similarly, the aforementioned methodology was applied to the faeces-contaminated sample. Again, principal component analysis was first performed to see the general trend of the spectra and to discover whether it is possible to discriminate among these three classes (fat, lean and contaminated surfaces) or not. The results were very promising and revealed that it is basically possible to distinguish these classes as shown in Figure 31 Figure 26.

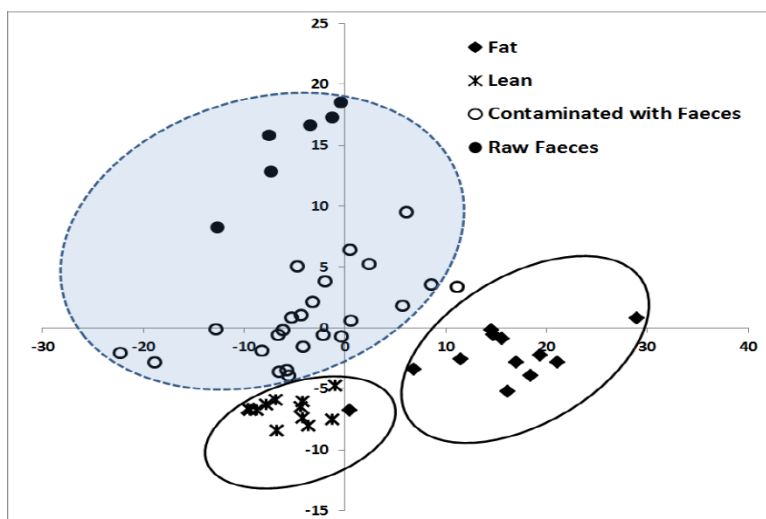


Figure 31 - PCA result for faeces (mean spectra)

As with the analysis of the ingesta spectral data, a number of spectra were extracted from hundreds of pixels representing the three classes (fat, lean and faeces contaminated surfaces). For the faeces-contaminated samples, this dataset consisted of 1784 spectra (329 fat spectra, 441 lean spectra and 1014 faeces spectra) collected from control and contaminated surfaces. First, the analysis was performed over the full spectral range of 400-2500 nm. Robust segmentation in this case was found to be difficult given the interactions between the spectral data of lean meat and faeces contamination, as shown by the red arrow in Figure 32.

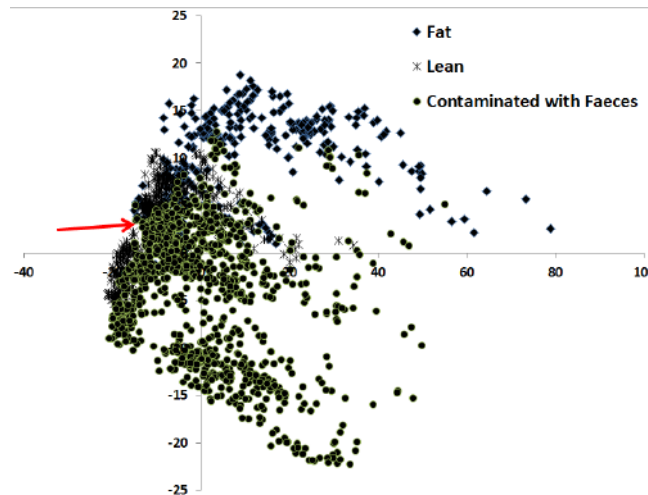


Figure 32 - PCA based on pixel spectra collected from control and contaminated samples with different concentrations of faeces

As aforementioned, there is little information carried in the 1400-2500nm spectral range. Thus, the PCA was repeated focussing on 400-1450nm. As a result, it can be seen that the accuracy of the discrimination improved significantly (Figure 33).

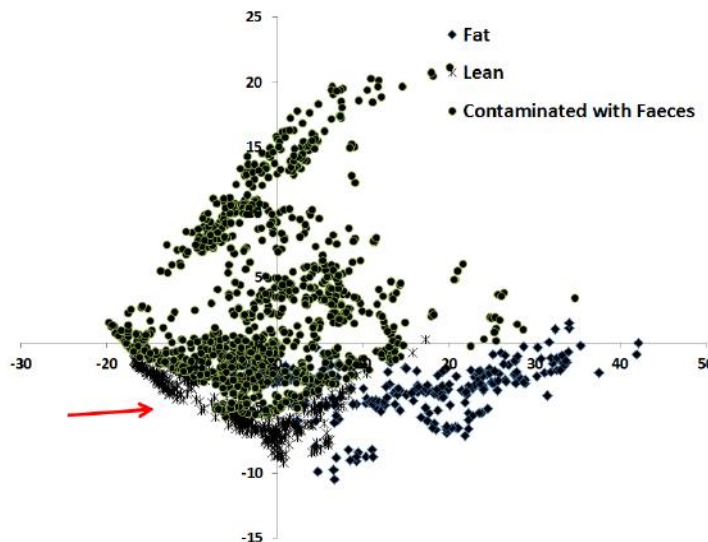


Figure 33 - PCA based on pixel spectra collected from control and contaminated samples with different concentrations of faeces in the spectral range 400-1450nm

Again, the PCA results were further refined by using the above results to select a number of key wavelengths. The classification accuracy was further improved when only 9 wavelengths out of the 362 available were selected (Figure 34).

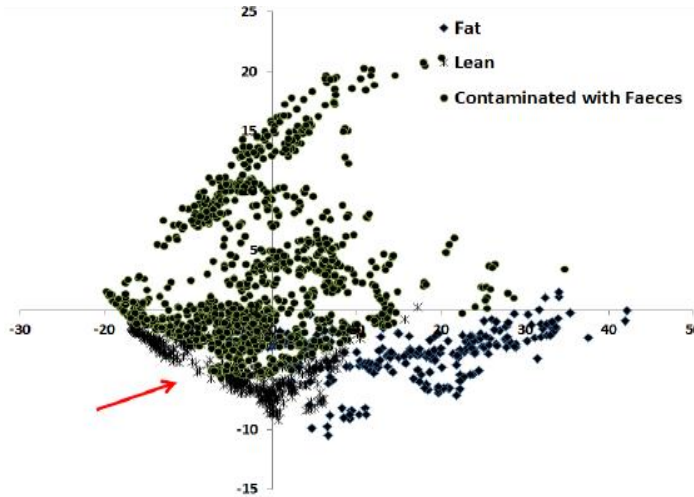


Figure 34 - PCA analysis for faeces (using key wavelengths)

Again, it can be noted that some interactions still exist, as indicated by the red arrow in Figure 34. Thus, a multivariate calibration model based on discriminant analysis was that used to not only classify the extracted spectra, but also to recognise the identity of every single pixel in the images. While this method works quite well for ingesta, it failed to produce meaningful results when applied to the faeces contamination data.

As with ingesta, a new discriminant analysis was then developed employing 11 key wavelengths along with two band ratios. The results, shown in Table 6, demonstrate a high level of accuracy in classifying the pixel data into the different categories of uncontaminated fat, uncontaminated lean and faeces-contaminated tissue.

Table 6 - Faeces classification result (pixel spectra) – 11 key wavelengths

from \ to	Fat	Lean	Faeces	Total	% correct
Fat	328	0	1	329	99.70%
Lean	0	441	0	441	100.00%
Faeces	4	0	1010	1014	99.61%
Total	332	441	1011	1784	99.72%



The model was then applied to every pixel in the images (Figure 35).

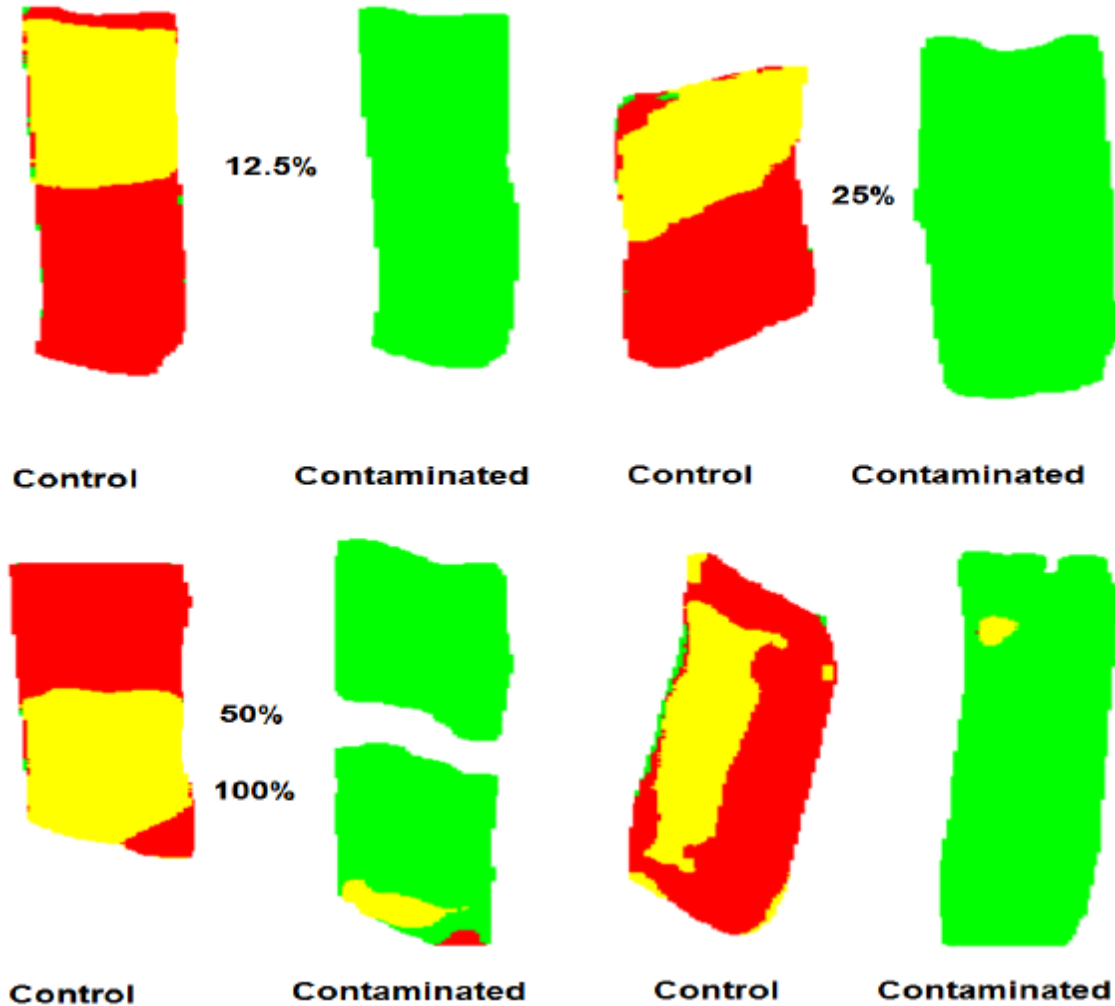


Figure 35 - Classification images of control and contaminated beef samples. Green indicates contamination with faeces, Red indicates uncontaminated lean meat, Yellow indicates uncontaminated fat. Note the presence of some green pixels on some of the control samples which indicates false positive matching for contamination for the current algorithm.

#### 5.4.3 Combined model

Ideally, one model would exist for the classification of a number of contaminants, including faeces and ingesta. A common model for faeces and ingesta was thus developed to examine the feasibility of such an approach. The two datasets were thus concatenated to give 4206 spectra and one model was developed using the eleven selected wavelengths and two band ratios to classify pixels as either uncontaminated lean, uncontaminated fat, ingesta-contaminated or faeces-contaminated. The results, shown in Table 7, demonstrate that a high level of classification can be achieved using such a method, especially considering that



misclassification between uncontaminated lean and uncontaminated fat is acceptable as they are both uncontaminated tissue.

Table 7 – Confusion matrix showing performance of the combined model for detecting faeces and ingesta contamination.

from \ to	Fat	Lean	Ingesta	Faeces	Total	% correct
<b>Fat</b>	847	44	0	1	892	94.96%
<b>Lean</b>	17	1005	0	48	1070	93.93%
<b>Ingesta</b>	0	0	1226	7	1233	99.43%
<b>Faeces</b>	6	10	3	992	1011	98.12%
<b>Total</b>	870	1059	1229	1048	4206	96.77%

In reality, faeces and ingesta can also be merged into one common ‘contaminant’ category. Such a model may then be relevant for other forms of contamination as well, although controlled trials as described in this report would need to be performed to confirm this. As can be seen in Table 8, the model results in an overall accuracy of 96.93% with an accuracy of 99.15% in detecting contaminant for a given pixel.

Table 8 – Confusion matrix showing performance of the combined model for detecting contamination.

from \ to	Fat	Lean	Contaminant	Total	% correct
<b>Fat</b>	849	43	0	892	95.18%
<b>Lean</b>	22	1003	45	1070	93.74%
<b>Contaminant</b>	6	13	2225	2244	99.15%
<b>Total</b>	877	1059	2270	4206	96.93%

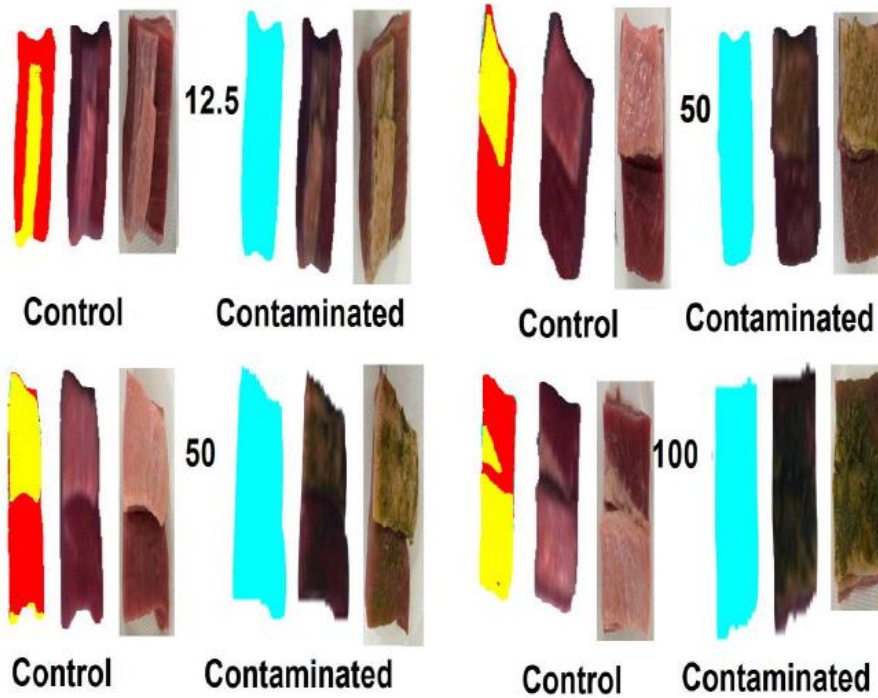


Figure 36 - Classification images for detecting **ingesta** using the combined model. Cyan indicates contamination, Red indicates uncontaminated lean meat, Yellow indicates uncontaminated fat.

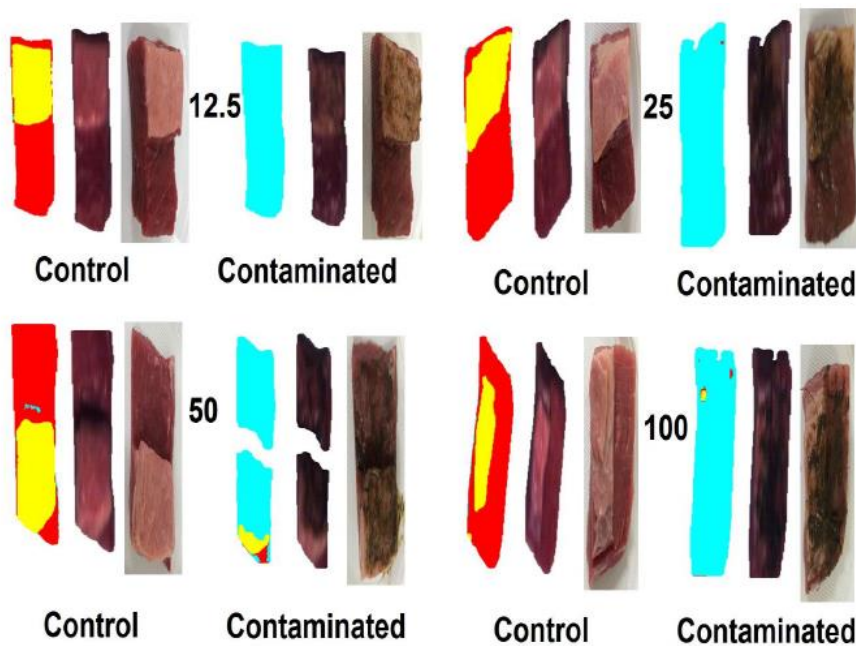


Figure 37 - Classification images for detecting **faeces** using the combined model. Cyan indicates contamination, Red indicates uncontaminated lean meat, Yellow indicates uncontaminated fat. Note, the middle portion missing from the 50% sample was caused by incorrect scanning resulting in some shadowing.

#### 5.4.4 Conclusions

Alternative methods of analysis also demonstrate a high-level of confidence that a system may be designed for automated detection of faeces and ingesta contamination using hyperspectral or multispectral technology. Furthermore, a general solution detecting any form of contamination may also be feasible using the methods outlined. One key outcome is the fact that these algorithms demonstrated an ability to flag contamination on a pixel-by-pixel basis. As should be the case, the algorithms highlighted the vast majority of the surfaces for each sample, even for the pixels in which contamination isn't visible to the naked eye.

## 6 Conclusions and Recommendations

This project saw the successful assessment of hyperspectral camera technology for the purposes of detecting contamination in red meat processing. An appropriate hyperspectral camera was selected and purchased. The model selected possesses a large spectral range which gives the greatest flexibility in identifying which wavelengths are of interest for any particular application.

A series of controlled experiments were then performed to investigate the following food safety concerns: ingesta, faeces, urine, bile, Salmonella, E. coli and Listeria. First, a number of samples of 'clean' meat was taken from the same herd and in the same area of the carcass to characterise the amount of natural variation in lean meat and fat spectra. The variation was found to be significant but a number of common features were able to be identified. Trials investigating the identification of varying amounts of contamination were then conducted. A key interest is detecting contamination levels which are invisible to the naked eye and this was taken into account with the methodology. Ultraviolet (UV) lighting also presents an opportunity area as some substances fluoresce when excited with UV light. Trials were thus conducted using UV light as well as standard white lighting to assess whether this could assist in the applications being explored.

After initial testing, the ingesta and faeces samples gave quite positive results. Urine and bile detection was possible in very high concentrations, but became difficult after a short amount of time, which then is absorbed into the sample. Further trials would have to be conducted but it is felt there is some potential in this area. Tests of the microbiological samples were also challenging once placed on the surface of meat samples, particularly at lower concentrations. One potential opportunity may be in performing time-lapsed trials of the contaminated samples.

It was then decided to perform more detailed trials investigating ingesta and faeces contamination. Control samples were taken of lean and fat which were then coated in various concentrations of faeces and ingesta contamination. The results were then analysed and algorithms using two different methods, a decision tree analysis and discriminant multivariate analysis. Both methods yielded high levels of accuracy in identifying both forms of contamination, even at the most diluted level of 12.5%. The latter method may possibly be able to identify any non-specific contamination.

It is therefore recommended that the results obtained in this project are built upon for further trialling work examining the detection of ingesta and faeces with a larger sample set. This sample set would cover a number of factors which may affect successful contamination detection, such as breed, diet, gender etc. Further work should be done in accurately comparing the system's performance with what is detectable to the naked eye. While there are portions of each sample where contamination isn't visible to the eye, the trialling methodology could be improved to further accentuate this. This may involve weighing samples of ingesta and faeces before drying them, crushing them up and dissolving them back into water. This would remove the large, fibrous portions of the contaminants. Alternatively, it may be possible to sieve samples to achieve the same result. From this work, the algorithms would be further tested and improved upon. A commercially feasible camera which possesses the ideal specifications for this application should also be defined along with a concept of what a commercial ingesta and faeces detection system might look like.

## Appendix A – Initial trial Results Register

Description	Contaminant	Concentration	Lighting Condition	VNIR exposure	SWIR exposure	Confidence (out of 10)	Notes Conclusion
Meat contaminated with Salmonella	salmonella	2x10 <sup>5</sup> cfu/ml	UV	31.8ms	28.9ms	3	at first glance it is not detectable, however further investigation is necessary
Meat contaminated with Salmonella	salmonella	2x10 <sup>5</sup> cfu/ml	White	17.8ms	5.9ms	3	at first glance it is not detectable, however further investigation is necessary
Meat contaminated with Salmonella	salmonella	376 cfu/ml	UV	31.8ms	28.9ms	3	at first glance it is not detectable, however further investigation is necessary
Meat contaminated with Salmonella	salmonella	376 cfu/ml	White	17.8ms	5.9ms	3	at first glance it is not detectable, however further investigation is necessary
Salmonella on conveyor	salmonella	2x10 <sup>5</sup> cfu/ml	UV	31.8ms	28.9ms	5	there are some minor spectral trends indicating that this differs from clean media, however further investigation is necessary
Salmonella on Spectralon	salmonella	2x10 <sup>5</sup> cfu/ml	UV	31.8ms	28.9ms	5	there are some minor spectral trends indicating that this differs from clean media, however further investigation is necessary
Salmonella on Spectralon	salmonella	2x10 <sup>5</sup> cfu/ml	White	17.8ms	5.9ms	5	there are some minor spectral trends indicating that this differs from clean media, however further investigation is necessary
Salmonella on conveyor	salmonella	2x10 <sup>5</sup> cfu/ml	White	17.8ms	5.9ms	5	there are some minor spectral trends indicating that this differs from clean media, however further investigation is necessary
Salmonella on conveyor	salmonella	10 cfu/ml	UV	31.8ms	28.9ms	5	there are some minor spectral trends indicating that this differs from clean media, however further investigation is necessary
Salmonella on Spectralon	salmonella	10 cfu/ml	UV	31.8ms	28.9ms	5	there are some minor spectral trends indicating that this differs from clean media, however further investigation is necessary
Salmonella on Spectralon	salmonella	10 cfu/ml	White	17.8ms	5.9ms	5	there are some minor spectral trends indicating that this differs from clean media, however further investigation is necessary
Salmonella on conveyor	salmonella	10 cfu/ml	White	17.8ms	5.9ms	5	there are some minor spectral trends indicating that this differs from clean media, however further investigation is necessary
Listeria on meat	listeria	212 cfu/ml	UV	31.8ms	28.9ms	3	at first glance it is not detectable due to the very small concentration of contaminant, however further investigation is necessary
Listeria on meat	listeria	212 cfu/ml	White	17.8ms	5.9ms	3	at first glance it is not detectable due to the very small concentration of contaminant, however further investigation is necessary
Listeria on Spectralon	listeria	212 cfu/ml	UV	31.8ms	28.9ms	5	there are some minor spectral trends indicating that this differs from clean media, however further investigation is necessary
Listeria on conveyor	listeria	212 cfu/ml	UV	31.8ms	28.9ms	5	there are some minor spectral trends indicating that this differs from clean media, however further investigation is necessary
Listeria on Spectralon	listeria	212 cfu/ml	White	17.8ms	5.9ms	5	there are some minor spectral trends indicating that this differs from clean media, however further investigation is necessary
Listeria on conveyor	listeria	212 cfu/ml	White	17.8ms	5.9ms	5	there are some minor spectral trends indicating that this differs from clean media, however further investigation is necessary
E.coli on meat	E.coli	10 <sup>5</sup> cfu/ml	UV	31.8ms	28.9ms	3	at first glance it is not detectable due to the very small concentration of contaminant, however further investigation is necessary
E.coli on meat	E.coli	10 <sup>5</sup> cfu/ml	White	17.8ms	5.9ms	3	at first glance it is not detectable due to the very small concentration of contaminant, however further investigation is necessary
E.coli on meat	E.coli	10 <sup>4</sup> cfu/ml	UV	31.8ms	28.9ms	3	at first glance it is not detectable due to the very small concentration of contaminant, however further investigation is necessary
E.coli on meat	E.coli	10 <sup>4</sup> cfu/ml	White	17.8ms	5.9ms	3	at first glance it is not detectable due to the very small concentration of contaminant, however further investigation is necessary
E.coli on meat	E.coli	16 cfu/ml	UV	31.8ms	28.9ms	3	at first glance it is not detectable due to the very small concentration of contaminant, however further investigation is necessary
E.coli on meat	E.coli	16 cfu/ml	White	17.8ms	5.9ms	3	at first glance it is not detectable due to the very small concentration of contaminant, however further investigation is necessary
E.coli on Spectralon	E.coli	16 cfu/ml	UV	31.8ms	28.9ms	5	there are some minor spectral trends indicating that this differs from clean media, however further investigation is necessary
E.coli on conveyor	E.coli	16 cfu/ml	UV	31.8ms	28.9ms	5	there are some minor spectral trends indicating that this differs from clean media, however further investigation is necessary
E.coli on Spectralon	E.coli	16 cfu/ml	White	17.8ms	5.9ms	5	there are some minor spectral trends indicating that this differs from clean media, however further investigation is necessary
E.coli on conveyor	E.coli	16 cfu/ml	White	17.8ms	5.9ms	5	there are some minor spectral trends indicating that this differs from clean media, however further investigation is necessary
E.coli on Spectralon	E.coli	10 <sup>4</sup> cfu/ml	UV	31.8ms	28.9ms	5	there are some minor spectral trends indicating that this differs from clean media, however further investigation is necessary
E.coli on conveyor	E.coli	10 <sup>4</sup> cfu/ml	UV	31.8ms	28.9ms	5	there are some minor spectral trends indicating that this differs from clean media, however further investigation is necessary
E.coli on Spectralon	E.coli	10 <sup>4</sup> cfu/ml	White	17.8ms	5.9ms	5	there are some minor spectral trends indicating that this differs from clean media, however further investigation is necessary
E.coli on conveyor	E.coli	10 <sup>4</sup> cfu/ml	White	17.8ms	5.9ms	5	there are some minor spectral trends indicating that this differs from clean media, however further investigation is necessary
E.coli on conveyor	E.coli	10 <sup>5</sup> cfu/ml	UV	31.8ms	28.9ms	5	there are some minor spectral trends indicating that this differs from clean media, however further investigation is necessary
E.coli on conveyor	E.coli	10 <sup>5</sup> cfu/ml	White	17.8ms	5.9ms	5	there are some minor spectral trends indicating that this differs from clean media, however further investigation is necessary
E.coli on Spectralon	E.coli	10 <sup>5</sup> cfu/ml	White	17.8ms	5.9ms	5	there are some minor spectral trends indicating that this differs from clean media, however further investigation is necessary
stainless steel with E.coli	E.coli	10 <sup>5</sup> cfu/ml	UV	31.8ms	28.9ms	2	further investigation is necessary
stainless steel with E.coli	E.coli	10 <sup>5</sup> cfu/ml	White	17.8ms	5.9ms	2	further investigation is necessary
stainless steel with E.coli	E.coli	10 <sup>4</sup> cfu/ml	UV	31.8ms	28.9ms	2	further investigation is necessary
stainless steel with E.coli	E.coli	10 <sup>4</sup> cfu/ml	White	17.8ms	5.9ms	2	further investigation is necessary
stainless steel with E.coli	E.coli	16 cfu/ml	UV	31.8ms	28.9ms	2	further investigation is necessary
stainless steel with E.coli	E.coli	16 cfu/ml	White	17.8ms	5.9ms	2	further investigation is necessary
50% ingesta contamination on meat	Ingesta	50%	White	17.8ms	5.9ms	10	detectible on this sample. The ability to detect low concentrations is limited by the spatial resolution of the camera

## P.PSH.747 – Hyperspectral Food Safety Inspection System

50% ingesta contamination on meat	Ingesta	50%	UV	31.8ms	28.9ms	10	detectible on this sample. The ability to detect low concentrations is limited by the spatial resolution of the camera
100% ingesta contamination on meat	Ingesta	100%	UV	31.8ms	28.9ms	10	detectible on this sample. The ability to detect low concentrations is limited by the spatial resolution of the camera
100% ingesta contamination on meat	Ingesta	100%	White	17.8ms	5.9ms	10	detectible on this sample. The ability to detect low concentrations is limited by the spatial resolution of the camera
12.5% faeces contamination on meat	faeces	12.50%	UV	31.8ms	28.9ms	8	with a higher spatial resolution camera, it would be possible to detect this contamination.
12.5% faeces contamination on meat	faeces	12.50%	White	17.8ms	5.9ms	8	with a higher spatial resolution camera, it would be possible to detect this contamination.
25% faeces contamination on meat	faeces	25%	UV	31.8ms	28.9ms	9	detectible on this sample. The ability to detect low concentrations is limited by the spatial resolution of the camera
25% faeces contamination on meat	faeces	25%	White	17.8ms	5.9ms	9	detectible on this sample. The ability to detect low concentrations is limited by the spatial resolution of the camera
50% faeces contamination on meat	faeces	50%	White	17.8ms	5.9ms	10	detectible on this sample. The ability to detect low concentrations is limited by the spatial resolution of the camera
50% faeces contamination on meat	faeces	50%	UV	31.8ms	28.9ms	10	detectible on this sample. The ability to detect low concentrations is limited by the spatial resolution of the camera
100% faeces contamination on meat	faeces	100%	White	17.8ms	5.9ms	10	detectible on this sample. The ability to detect low concentrations is limited by the spatial resolution of the camera
100% faeces contamination on meat	faeces	100%	UV	31.8ms	28.9ms	10	detectible on this sample. The ability to detect low concentrations is limited by the spatial resolution of the camera
fat in urine	Urine	Unknown	UV	31.8ms	28.9ms	2	Further investigation is necessary to examine the fluorescence of urine on fat
ingesta on fat	ingesta	Unknown	UV	31.8ms	28.9ms	2	Further investigation is necessary to examine the fluorescence of ingesta on fat
fat in Bile	bile	Unknown	UV	31.8ms	28.9ms	2	Further investigation is necessary to examine the fluorescence of bile on fat
faeces on fat	faeces	Unknown	UV	31.8ms	28.9ms	2	Further investigation is necessary to examine the fluorescence of faeces on fat
faeces on fat	faeces	Unknown	White	17.8ms	5.9ms	10	detectible on this sample. The ability to detect low concentrations is limited by the spatial resolution of the camera
ingesta on fat	ingesta	Unknown	White	17.8ms	5.9ms	10	ingesta is detectible on this scan. The ability to detect low concentrations is limited by the spatial resolution of the camera
fat in Bile	bile	Unknown	White	17.8ms	5.9ms	5	bile is detectible in large concentrations on fat and meat, but is absorbed quickly after application and becomes undetectable
Urine on fat	Urine	Unknown	White	17.8ms	5.9ms	1	the spectra of meat and fat does not appear to be changed with the application if urine on the surface
E.coli on Spectralon	E.coli	10 <sup>5</sup> cfu/ml	UV	31.8ms	28.9ms	5	there are some minor spectral trends indicating that this differs from clean media, however further investigation is necessary